5.3.7 Available and expected EM facilities characteristics

In figure 100 we report the results of a survey within the ET observational science board on the best EM current facilities and future projects for multi-messenger observations (column 1), as well as their corresponding characteristics, in terms of Field of View (FoV; column 2), sensitivity (column 3), spectral range (column 4), resolution (column 5), capability and time delay to perform Target of Opportunity (ToO) (column 6), survey strategy (column 7), data policy and data access (columns 8 and 9). Each facility may be of good use to look and/or to follow-up and characterize one or more type of EM counterparts (GRBs, off-axis afterglows, KNe). This is indicated from column 10 to 15. Projects that are still at the proposal stage and not yet adopted are indicated with an asterisk.

5.3.8 Requirements for ET BNS and BHNS multi-messenger observations based on simulations.

Based on the simulations presented in this work, in figures 101–103 we report the minimal requirements to detect and study the EM counterparts (on-axis GRB, off-axis afterglow, KN) of BNS and BHNS detected by ET, for EM facilities working in different ranges of the EM spectrum. The evaluation of the requirements takes into account a balanced amount of time to be required to the EM observatories. We consider the FoV, sensitivity, spectral range, resolution, and capability and time delay to perform ToOs. We separate the *Search* for the EM candidate counterparts (orange columns) from their in depth study for the *Characterization* of their properties (green columns). For on-axis GRBs, the search requirements are based on the assumption of a GRB prompt detection by a satellite with arcmin localization capability. For the VHE the requirements take into account the possibility to point pre-merger to detect the emission during the prompt/early phase. We stress that, except for the scenario of a well-localized GRB detection in temporal coincidence with a GW signal which can drive the multi-wavelength search and characterization, also in the ET era sensitive wide FoV instruments ($> 1\,\mathrm{deg}^2$) will be necessary for the search. In addition, to increase the chance to detect off-axis afterglows also observations at late time (months to years) might be required. Except for on-axis GRBs, very sensitive instruments are required at any wavelength for the characterization.

5.4 Neutrinos from Compact Binary Coalescence

5.4.1 Common environments for neutrinos and GWs

The existence of a common astrophysical source of neutrinos and GWs is theoretically well-motivated. One such example is compact binary mergers. The most promising ones are binary systems with at least one neutron star component, such as binary neutron stars (BNS), and neutron star-black hole (NSBH) systems [2368–2370]. Otherwise, binary black holes (BBH) embedded in Active Galactic Nuclei (AGN) disks could also have a favourable environment for neutrino production [2371, 2372].

Based on theoretical predictions, following the merger, a central compact object is formed. Consequently, powerful relativistic jets efficiently eject the remaining accretion disc matter into the surrounding environment after the merging phase. There, non-thermal charged

JCAP03(2026)081

	FoV (deg) -diam	Sensitivity	Spectral range	Resolution (spectral / spatial)	ToO? delays?	Survey strate	Data policy	Data access	search	characterization	On-axis GRB/ afterglow	off-axis GRB /afterglow	KN
SKA-MID	1 degree * (1.4 GHz/observing freq)	1-4 uJy in one hour	0.35-15.4 GHz	Channel width 13-80 kHz, up to 200 Hz 'zoom' Angular: 0.4 arcsec * (1.4 GHz/frequency)	Transient buffers 288 sec / ToO or DDT likely	not yet clear	not yet published, but imminent		X	X	X	X	
SKA-LOW	2 degrees * (300 MHz/observing freq)	14-26 uJy in one hour	0.05-0.35 GHz	Channel width 5 kHz, up to 220 Hz 'zoom' Angular: 6-300 arcsec	Likely transient buffers / Likely ToO or DDT policy	not yet clear	not yet published, but imminent		X	X	X	X	
ngVLA	0.6 - 25 arcmin (from top to bottom of spectral range)	0.15-0.40 uJy/beam in one hour	1.2-50.5 GHz and 70-116 GHz	Narrowest channel < 1 kHz; Angular: 1 milliarcsec - 1 arcsec; LBA to 0.1 milliarcsec	Likely ToO and/or DDT policy	TBD	not yet published	NRAO archive		X	'X	X	
ALMA 2030 (WSU)	19" at 300 GHz for a 12-m antenna and a 33" for a 7-m antenna for single pointings	Continuum sensitivity in one hour: 2 uJy/beam and 0.3 mJy/beam at 40 and 950 GHz, respectively.	35-950 GHz	Spectral: 13.5 kHz resolution over full receiver bandwidth (velocity resolution of 0.12 (35 GHz/v)km s−1, where v is the observed frequency in GHz). Ultra-high resolution of 10 m/s with zoom mode at all frequencies. / Spatial:	Y, reaction time can be less than 24 hours but depends on several factors		Proprietary	Public archive		X	X	X	
AtLAST	2 degrees (circular, 2 instrument slots with this FoV) or 1 degrees (4 instrument slots with this FoV). Note the higher frequencies (>400) will be closer to < 1 degree with the optical corrections.	Continuum (over delta\nu=18 GHz bandwidth) = 180 microJy/beam in 60seconds at 300 GHz observing frequency (assuming 25th percentile weather conditions and 60 deg elevation), beam is 4.3" at this frequency.	30 - 950 GHz (over approximately 8 broad windows where the Earth's atmosphere is transparent)	Spatial: under diffraction-limited assumption, FWHM arcsec ~ 1300/obs_frequency(GHz) or FWHM arcsec = lambda(microns)/230. Spectral: depends on instrument, from resolutions of R 10^7 (heterodyne) to R 300 for (sub)mm-IFUs, and to broadband (~40 GHz per band) continuum multi-chroic bolometer/KID arrays.	ToO yes		Proprietary for 1year	Public archive	X	X	X	X	
BLACKGEM	8.1 deg^2 (3 x 2.7 sq. deg)	q(white) = 23 is 300s (dark)	350-1000nm	arcsec									
GOTO	2 x 100 deg^2 (North/South)	L(white)=21 in 60s (dark)	450-1000nm	~ 1300/obs_frequency(GHz) or									
Rubin Observatory	1.75 degrees (9.6 sq. deg. effective FoV)	r=24.0 mag in 30s	ugrizy filters (~3,500-10,000A)	arcsec	ToO yes	TBD	public alerts; images avaiable after 80 hours to member countries	via Alert Brokers; Rubin Science Platorm https://data.lsst	X	X	X	X	X
WFST	~6 sq. deg. effective FoV	r=22.84 mag in 30s	ugrizw filters (~3,500-9,000A)	=	ToO yes	Deep High-cadence Survey and Wide-field Survey	Proprietary	private pipeline	X	X	X	X	X
ELT/HARMONI	Four different FoVs: 0.61"x0.82"; 1.52"x2.04"; 3.04"x4.08"; 4.56"x6.12"	5hr on-source integration, SNR=5: R_AB=23 (4mas/px scale), 25 (30mas/px); H_AB=26.3 (4mas/px, R=3100), 24.3 (4mas/px, R=17000) , 26.8 (30mas/px, R=3100), 25.2 (30mas/px, R=17000); K_AB=25.7 (4mas/px, R=3100), 24.4 (4mas/px, R=17000) , 25 (30mas/px, R=3100), 24.4	(0.47) 0.8 - 2.45 um		TBD	N/A	TBD	ESO archive		X		X	X
ELT/MICADO-lma	LR: 50 arcsec (0.014 deg diameter), HR: 19 arcsec (0.0053 diameter)	5 hr, 5 sigma limiting point source AB mag: J~28.6, H~29.5, K~29.1	I,Y,J,H,K filters	lambda(microns)/230.	TBD	N/A	TBD	ESO archive		X		X	X
ELT/MICADO-Spec	Slit (width x length): 16masx3", 20masx15", 48masx3"	similar to imaging mode	1.4-2.46 um or 0.96-1.55 um	Spectral: ~10000 or ~20000	TBD	N/A	TBD	ESO archive		X		X	X
ELT/MOSAIC	Patrol field of 40 arcmin2 with 3 obsvering modes: - MOS-VIS: 140 VIS apertures of 0.7" at LR, 85 apertures at HR - MOS-NIR: 200 NIR apertures of 0.6" at both LR and HR - NIR-mIFU: 8 hexagonal NIR IFUs of 2.2arcsec diameter Possible parallel observations mixing VIS and NIR apertures/IFUs in the patrol field	Performances currently in revision/estimation following a recent evolution of the architecture. Examples of objectives: -point sources at LR with MOS modes: I(AB)~24.5 with S/N >=20, V(AB)~22 with S/N>=50, H(AB)~25.4 with S/N>=20 -extended sources at LR with MOS modes: R(AB)=25.5 with S/N>=4, H(AB)=23.5 with S/N > 20/A -extended sources at LR with IFUs: J(AB)=26-27 with S/N>3 per spaxel in emission lines	VIS: 380-950 nm in three bands obtained in one shot NIR= 950-1800 nm in two bands obtained in one shot	VIS-LR at R>=4,000 NIR-LR at R>=4,000 4 VIS-HR windows at R>=18,000: 390-450, 510-590, 610-710, 800-940 (all TBC) 1 NIR-HR window at R>=18,000: 1520-1670 (TBC) For the NIR-IFUs: spaxel scale = 150mas	TBD	TBD	TBD	ESO archive	X	X		X	X
ELT/ANDES seeing-limited	1 square-arcsec	AB=20 in 1 hr SNR=10	400-1800 nm	R=100,000	yes	N/A	tbd	ESO archives		X	X		
ELT/ANDES IFU	0.5 square-arcsec	AO requires m(_AB)=6-15mag	980-1800 nm	R=100,000	yes	N/A	tbd	ESO archives					
VLT/MUSE-GLAO or seeing limited	1 arcmin (0.017 deg diameter)	V(AB)=22, 1hr, SNR=5 (@550nm)	465.000 - 930.000 nm or 480.000 - 930.000 nm	Spatial: 250 mas per pixel, Spectral: 3000-3500	yes	N/A	0 to 12 months proprietary time	ESO archives		X	X		X
VLT/MUSE-LTAO	7.5 arcsec (0.0021deg diameter)	V(AB)=21.5, 1hr, SNR=5 (@550nm)	480.000 - 930.000 nm	Spatial: 25 mas per pixel, Spectral: 3000-3500	yes	N/A	0 to 12 months proprietary time	ESO archives		X	X		X
VLT/X-shooter	Slit length=13", several slit width (e.g., 0.5", 0.8", 1.0", 1.3", 1.6", 5.0"), depending on the arm	m_AB=22.4@500nm, m_AB=21@800nm, m_AB=20.5@1500nm, m_AB=19@2000nm in 1hr and with SNR=10	300-2500 nm split in 3 arms	Spectral resolution depends upon the selected slit, and the considered arm wavelength. Generally, it reanges from min 4300 to max 18400	yes	N/A	0 to 12 months proprietary time	ESO archives		X	X		
WST*	3 deg^2 MOS (3x3 arcmin IFS)	m_AB=24.5 MOS, m_AB=25.2 IFS in 1hr and with SNR=10	350-970nm to be extended to 1600nm	LR mode R=4000, 20000 fibers; HR mode R=40000, 2000 fibers	yes, ~hours	TBD	tbd	tbd	X	X			X
MSE*	1.5 deg^2	m_AB=24, 1hr	360-950 nm; 360-1800nm	3000 (NIR extension), 6500, with 20000 fibers; HR mode R=20000	foreseen, ?	TBD	tbd	tbd					
HST	variable by instrument (up to ~10 sq. arcmin)	r(F606w) ~ 29(AB)	100-1600 nm imaging and spectroscopy	0.1" resolution in imaging (wavelength dependent), low resolution grism (R~100) in optical/IR. Higher resolution available via COS and STIS (up to	Non-disruptive ToO: >21 days, Disruptive ToO 3-21 days, ultra-disruptive <3 days.								
JWST/NIRCam	9.7 arcmin²	m_AB=22 (grism), m_AB=29-31 depending on the configuration; S/N=10 in	2400-5000nm (grism), 600-5000nm covered by different filters	R~1600 / << 1 arcsec	Non-disruptive ToO: > 14 days; Disruptive ToO: between 3 and 14; Ultra-disruptive ToO: < 3	NA	0 to 12 months proprietary time	archive		X		X	X
JWST/NIRSpec	3"x3" in IFU mode	m_AB=26 (grism), m_AB=22-24 depending on the configuration; S/N=10 in	600-5000nm (prism), 700-5000 divided in 3 bands	R=100,1000, 2700 depending on the obs. mode	Non-disruptive ToO: > 14 days; Disruptive ToO: between 3 and 14; Ultra-disruptive ToO: < 3	NA	0 to 12 months proprietary time	archive		X		X	X
JWST/MIRI	112.6"x73.5"	m_AB=23 (slit @8000nm), m_AB=24 (imaging @13000nm) ; S/N=10 in	5000-12000nm (slit); 5600-25000nm (imaging, covered by different filters))	R~100 / <1 arcsec	Non-disruptive ToO: > 14 days; Disruptive ToO: between 3 and 14; Ultra-disruptive ToO: < 3	NA	0 to 12 months proprietary time	archive		X		X	X
JWST/NIRISS	133" × 133"	m_AB=25, m_AB=28 (imaging)	800-2200nm, 800-5000nm (imaging covered by different filters)	R~150 / << 1 arcsec	Non-disruptive ToO: > 14 days; Disruptive ToO: between 3 and 14; Ultra-disruptive ToO: < 3	NA	0 to 12 months proprietary time	archive		X		X	X
ROMAN	0.281 sq degree	m_AB=28 depending on the	500--2000nm	R=461 R= 80-180 depending on	TDAMM program	TBD	0 to 12 months	archive		X		X	X
SVOM/GRM	~5.6 sr combined, 3 modules of 2.6 sr	0.22 ph/cm2/s	15 keV-5 MeV	<16% @60 keV	Y, from <5 hours to 48 hours depending on urgency		Data are proprietary, scientific products public		X		X		
SVOM/ECLAIRs	2 sr	1.6 ph/cm2/s	4-120 keV	1.3 keV @60 keV, 12 arcmin (loc. accuracy)	Y, from <5 hours to 48 hours depending on urgency		Data are proprietary, scientific products public				X	X	
SVOM/VT	26'x26'	22.5 in 300 seconds	450-1000nm	~ arcsec	Y, from <5 hours to 48 hours depending on urgency		Data are proprietary, scientific products		X		X		
SVOM/MXT	~1 deg^2	~10^-12 erg/cm2/sec	0.2-10 keV	75 eV, ~ tens of arcsec	Y, from <5 hours to 48 hours depending on urgency		Data are proprietary, scientific products		X		X	X	
Swift/BAT	1.4-1.6 steradiants	0.3 ph/cm2/s **	15-150 keV	7 keV, 20 arcmin	yes, as soon as schedulable		Public	Public archive	X		X		
Swift/XRT	15'	8 x 10^-14 erg cm-2s-1 in 10^4	0.3-10 keV	190 eV (10KeV), 18 arcsec	yes, as soon as schedulable		Public	Public archive	X	X	X	X	
Einstein Probe	WXT: ~1.1 steradiants; FXT: 60 arcmin (diam)	WXT: 2.5x10^(-11) erg/cm2/s in 10^3 s FXT: ~.10^(-13) erg /cm2/s in 1500 s	WXT: 0.5-4.0 keV; FXT: 0.5-10 keV	WXT: ~3 arcmin (spatial) FXT: 5-15 arcsec (spatial)	yes, ass soon as schedulable	tiling, scan region	Proprietary		X	X	X		
AXIS*	24 arcmin (diameter)	1.5x10^(-15) erg cm-2s-1 in 10^	0.3-10 keV	< 2 arcsec	yes, ~ 2 hours	TBD	TBD	TBD	X	X	X	X	
NewATHENA*	40x40 arcmin^2 (WFI); 4 arcmin (diameter; IFU)	few 1e-16 erg/cm2/s (WFI) in 10^4s	0.2-12 keV	4 eV @ 7 keV / 5"	>12 hrs	tiling, scan region	TBD	TBD	X	X	X	X	
THESEUS/SXI*	0.5 steradiant	1e-10 erg/cm2/s (100 sec)	0.3-5 keV	<2 arcmin	Y, 0-15 min		TBD	Public archive	X	X	X	X	
THESEUS/XGIS*	2 steradiant	1e-8 erg/cm2/s	3kev-2MeV	15 arcmin	N		TBD	Public archive	X		X	X	
THESEUS/IRT*	15x15 arcmin	21(I) to 20.8(H) (150s, SNR=5)	0.7-1.8 mu	R~400	Y, 0-15 min		TBD	Public archive		X	X	X	X
FERMI/GBM	~8 steradiant	2 ph/cm2/s	8keV-40MeV	1-100 keV (0.01-10MeV),10 deg			Public	Public archive	X		X	X	
FERMI/LAT	2.5 sr	1e-6 erg/cm2/s	20 MeV - 300 GeV	3.5-0.15 deg (100 MeV-10GeV)			Public	Public archive			X		
HERMES Pathfinder	5.2 sr	5 ph/cm2/s	3keV-2MeV		No		TBD	Public archive	X		X	X	
HERMES Conts*	All sky	1 ph/cm2/s	3keV-2MeV		No		TBD	Public archive	X		X	X	
CTAO	3.5-11	1e-12 erg/cm2/s @100 GeV 50hrs; 5e-11 erg/cm2/s MAGIC-	20 GeV - 300 TeV	5-15%	20-40 s	tiling, scan region	TBD	Public interface (gammapy)	x		x		
LST	3.5	1e-12 erg/cm2/s @100 GeV 50hrs; 5e-11 erg/cm2/s MAGIC-	20 - 300 GeV	15-10%	20s	tiling, scan region	Proprietary	private pipeline	x		x		
ASTRI-MA	10	1e-10 erg/cm2/s @1TeV 100s	1-300 TeV	~10% >1 TeV; 0.05 deg	40s	tiling, scan region	Proprietary	private pipeline	x		x		

Figure 100. Characteristics of most advanced EM facilities expected to be available by the late 2030s. Also available as an Excel table at https://apps.et-gw.eu/tds/ql/?c=17760. Asterisk indicates facilities and missions that are still in the project phase and have not yet been approved or adopted.

ON-AXIS GRB and AFTERGLOW

	SEARCH					CHARACTERIZATION				
	FoV	Sensitivity	Spectral range (nm)	Spectral / Spatial Resolution	ToO delay	FoV	Sensitivity	Spectral range (nm)	Spectral / Spatial Resolution	ToO delay
Radio		0.1 mJy	> 1 GHz	-- / ~ 1"	hours	arcsec^2	0.01 mJy	> 1 GHz	--/~arcsec	monitoring Log scale
NIR	~ few arcmin^2	21 mag	1000 - 1800 nm	-- / ~ 1"	minutes	arcsec^2	24 mag (phot.) 22 mag (spectr.)	1000-1800 nm	low-mid / 1"	< 12 hr
Optical	~ few arcmin^2	22 mag	500 - 900 nm	-- / ~ 1"	minutes	arcsec^2	26 mag (phot.) 22 mag (spectr.)	300-900 nm		
X-ray	~ tens of arcmin^2	10^{-13} erg cm^{-2} s^{-1}	0.2-10 keV	a few arcsec	< hours	~ tens of arcmin^2	10^{-16} erg cm^{-2} s^{-1}	0.2-10 keV	a few arcsec	< hours
γ-ray	~10 sr	~1 ph cm^{-2} s^{-1}	10 keV - 10 MeV	arcmin						
VHE	>1 deg^2	< 10^{-10} erg cm^{-2} s^{-1}	10 GeV - 30 TeV	DE/E ~20% 0.1-1 deg	< hours	1 deg^2	< 10^{-11} erg cm^{-2} s^{-1} @100 GeV	10 GeV - 30 TeV	DE/E ~20% 0.1 deg	< hours

Figure 101. Minimal requirements for detecting and characterizing EM counterparts of BNS and BHNS mergers detected by ET, considering on-axis GRB and afterglow emission and EM facilities operating across different wavelength ranges. The gamma range in the table extends to the X-ray band considering the characteristics of the gamma-rays instruments for GRB detection.

OFF-AXIS AFTERGLOW

	SEARCH					CHARACTERIZATION				
	FoV	Sensitivity	Spectral range (nm)	Spectral / Spatial Resolution	ToO delay	FoV	Sensitivity	Spectral range (nm)	Spectral / Spatial Resolution	ToO delay
Radio	≥ 1 deg^2	< 10^{-2} mJy	> 1 GHz	--/~arcsec	Few days to years!	Some arcsec^2	< 10^{-3} mJy	> 1 GHz	--/~arcsec	logarithmic monitoring for days, months, years
NIR	≥ 1 deg^2	> 24 mag (AB) < 10^{-3} mJy	> 1000 nm	--/~arcsec	Few days to years!	~ arcsec^2	> 24 mag (AB) < 3×10^{-4} mJy	1000-1800 nm	low-mid / ~1"	ToO at first then logarithmic monitoring
Optical	≥ 1 deg^2	> 26 mag (AB) < 10^{-4} mJy	500 - 900 nm	--/~arcsec	Few days to years!	~ arcsec^2	> 27 mag (AB) < 5×10^{-5} mJy	500 - 900 nm	low-mid / ~1"	ToO at first then logarithmic monitoring
X-ray	≥ 1 deg^2	< 10^{-13} erg cm^{-2} s^{-1} < 10^{-7} mJy	0.2-10 keV	--/few arcsec	Few days to years!	~ arcsec^2	< 10^{-17} erg cm^{-2} s^{-1} < 10^{-8} mJy	0.2-10 keV	--/few arcsec	logarithmic monitoring for days, months, years
γ-ray	~10 sr	0.01-0.1 ph cm^{-2} s^{-1}	3 keV - 10 MeV	--/arcmin						

Figure 102. Minimal requirements for detecting and characterizing EM counterparts of BNS and BHNS mergers detected by ET, considering off-axis afterglow emission and EM facilities operating across different wavelength ranges. In this case, we consider a field of view equal to $1, \mathrm{deg}^2$ (for radio, NIR, optical, and X-ray), in contrast to figure 103, where a larger field of view is required. This choice accounts for the possibility of detecting gamma-ray or X-ray emission from slightly off-axis systems, which could enable source localization. The gamma range in the table extends to the X-ray band considering the characteristics of the gamma-rays instruments for GRB detection.

particles are accelerated in the presence of strong magnetic field. The accelerated protons in and around the jet actively participate in hadronic interactions. They interact with the strong ambient photon fields, leading to photo-pion interactions. As one of the secondary particles, high-energy neutrinos (HENs) are produced via charged pion decay. It could happen during the prompt phase [2373], and also later, coincident with the longer afterglow radiation [2374]. It is worth mentioning that HENs can also be produced via hadronuclear (pp) interactions. Such processes also result in the production of charged pions and kaons, which subsequently decay into charged leptons and neutrinos. Furthermore, neutral pions,

JCAP03(2026)081

KILONOVA

	SEARCH					CHARACTERIZATION					
	FoV	Sensitivity (AB)	Spectral range (nm)	Spectral / Spatial Resolution	ToO delay	FoV	Sensitivity (AB)	Spectral range (nm)	Spectral Res.	ToO delay	
NIR	>1 deg²	>22 mag	1000-1800	~1000 / ~ 1″	1 day	~arcsec²	>24 mag	1000-1800	>1000	1 day	Ideally nightly monitoring of the evolution for ~1week. However at such late time most counterparts will reach exteremely faint magnitudes (m~30 AB)
Optical	>1 deg²	>22 mag	500-900	~1000 / ~ 1″	12 hr	~arcsec²	>24 mag	500-900	>1000	12 hr	Ideally nightly monitoring of the evolution for ~1week. However at such late time most counterparts will reach exteremely faint magnitudes (m~30 AB)
UV	>1 deg²	>22 mag	300-500	~1000 / ~ 1″	< 1 hr	~arcsec²	>24 mag	300-500	>1000	< 1 hr	Ideally nightly monitoring of the evolution for ~2-3 days.

Figure 103. Minimal requirements for detecting and characterizing EM counterparts of BNS and BHNS mergers detected by ET, considering KN emission and EM facilities operating across different wavelength ranges.

produced from the same primary hadrons, decay into high-energy photons. These photons, if within the observable range from Earth, strengthen the connection between high-energy neutrinos and gravitational waves, reinforcing the multi-messenger approach.

5.4.2 Current and future neutrino telescopes

In view of promising theoretical predictions, since the last decade, multiple neutrino detectors have been looking for the correlation between the detection of gravitational waves and any possible detection of astrophysical neutrinos. At the time of writing, three major installations, IceCube, KM3NeT, and GVD-Baikal, are active and taking data although at different stages of realisation. All of them come with a target instrumented volume of the size of $1\,\mathrm{km}^3$.

The IceCube Neutrino Observatory [2375, 2376] completed its installation in 2013. It is a cubic kilometer ice-Cherenkov detector located under the Antarctic ice in the geographic South Pole. Motivated by its rich science output, further enhancements offering better sensitivity across a vast energy range are envisioned. The sensitivity of IceCube in the sub-TeV range will improve with the installation of IceCube Upgrade [2377, 2378], i.e. seven new densely packed strings, planned for 2025–26. Another extension of the existing IceCube infrastructure in planning is IceCube-Gen2 [2379]. It will be an $8\,\mathrm{km}^3$ and multi-component detector with better sensitivity to HENs with energies above 1 PeV.

Although already operational, KM3NeT and GVD-Baikal are still in construction stages in the abyssal site of the Mediterranean Sea and at the bottom of Baikal Lake in Siberia, respectively. In the Northern Hemisphere, the KM3NeT neutrino telescope [2380] is composed of two undersea detectors, namely ORCA and ARCA. KM3NeT/ARCA, with a target instrumented volume of $1\,\mathrm{km}^3$, is optimised for the detection of astrophysical neutrinos from 10 TeV up to hundreds of PeV. KM3NeT/ORCA is designed to study the physical properties of neutrinos, such as the mass hierarchy and the oscillation parameters, by detecting the atmospheric neutrinos in the sub-GeV up to the TeV energy range. Early in 2025, the KM3NeT Collaboration published the discovery of a record-breaking neutrino detected by

JCAP03(2026)081

KM3NeT/ARCA with an estimated energy of about 220 PeV [2381], demonstrating the excellent capabilities of underwater neutrino telescopes.

Baikal-GVD [2382] is located at a depth of $\sim$ 1400 m in the Baikal Lake. Promising results of the measurement of the astrophysical neutrino diffuse flux above 100 TeV were recently published [2383].

A group of next-generation TeV-PeV neutrino telescopes are under design. In some cases, the prototypes of the new technologies are already being tested. They are concentrated in the Northern Hemisphere in different sites around the World. P-ONE [2384], currently at a prototypal stage, aims at the realisation of a 1 km^3 array of multi-PMT optical modules off Canada in the Pacific Ocean. The Chinese project TRIDENT [2385] is studying the feasibility of a neutrino telescope in the South China Sea, aiming at an instrumented volume of 8 km^3. In China, other ambitious projects are under discussion (e.g. NEON [2386] or HUNT [2387]) to realise very large telescopes of 10 km^3 or 30 km^3.

Binary neutron star mergers are potential sources of ultrahigh-energy neutrinos (above 1 PeV), and next-generation radio detectors such as GRAND [2388], IceCube-Gen2 Radio array, and RNO-G [2389] are designed to detect these elusive particles.

5.4.3 Multi-messenger neutrino and GW frameworks

Despite all the decade-long observational efforts, coincident detection of HEN and GWs is still missing [2293, 2390–2393]. To date only upper limits on the HEN content of GRBs [2394] and observed GW sources have been obtained, owing, most likely to the fact that the current neutrino experiments are not sensitive enough to the neutrino flux of individual sources.

At present, both IceCube and KM3NeT are following up on the existing individual GW events to identify their neutrino counterparts. The current GW follow-up strategy consists of both real-time and archival searches for individual GW events, using different event topologies, ranging from MeV to PeV energies [2395–2399]. Sub-threshold GW events from the Ligo-Virgo-KAGRA third observation run (O3) are also separately followed up by IceCube in an archival search to identify potentially interesting multi-messenger sources [2400]. Similar studies would play a crucial role in the era of next-generation GW detectors. For GeV-TeV neutrinos, the typical observation time window is selected to be $\pm$ 500 s concerning the GW event detection time. We expect the neutrino signal from the source to dominate over the background within this time window [2401, 2402]. However, in IceCube, for BNS mergers, an extended time window of two weeks is also considered, to account for certain model predictions [2403]. Additionally, real-time analysis to identify MeV neutrino bursts with IceCube within four different time windows: 0.5 s, 1.5 s, 4 s, and 10 s associated with individual GW events is under development [2395]. On the other hand, in KM3NeT, an additional [-500 s, +6 h] time window is considered for real-time searches of GeV-TeV neutrinos, while a 2 s window is used for MeV neutrinos. So far, no significant correlation has been observed. An alternative archival search strategy could also be explored in the future, aiming to identify neutrino counterparts from a population of GW candidates via stacking analysis. This approach enhances the detection potential by accumulating signal neutrinos within an optimal time window, allowing them to stand out against the background neutrino distribution.

JCAP03(2026)081

Such observational prospects will surely increase with next-generation GW like Einstein Telescope (ET) and HEN detectors, specifically with KM3NeT, and Baikal-GVD. Once they reach their nominal size and with the active participation of P-ONE and IceCube-Gen2, the combined performance of all these advanced neutrino detectors can offer maximum sensitivity to detect neutrino sources all over the sky, which would benefit GW follow-up efforts [2404]. According to the current plan, the Einstein Telescope [15, 16] and the US-lead Cosmic Explorer (CE) [13, 14] will be able to detect BNS mergers out to O(10) Gpc. During their active operation time, IceCube and KM3NeT will continue actively participating in the GW follow-up efforts. As neutrinos do not get absorbed or deflected while propagating toward us from the respective astrophysical sources, the prospect of coincident detections from the furthest of sources in the future remains a key objective. With the expected boosts in the sensitivities of future neutrino detectors, extending the current searches for coincident detection of HEN and GWs for next-generation detectors is crucial for the future of multi-messenger astronomy. Ref. [2405] investigates the prospects of performing triggered-stacking searches for coincident high-energy neutrinos from BNS mergers, using next-generation GW detectors in synergy with IceCube-Gen2. The study quantifies optimal distance thresholds and time windows to minimize background, and highlights that precise sky localization, achieved by the combined network of ET and CE, is essential for enabling either neutrino detections or placing meaningful constraints on emission models within approximately 10 years. A fraction of BNS mergers is expected to produce long-lived magnetars as remnants, which, according to some models, can lead to enhanced electromagnetic and neutrino emission. Ref. [2406] shows that GW-triggered stacking searches, using the ET and CE network together with IceCube-Gen2, offer a realistic chance of detecting neutrinos from these events within an operational timescale of about 20 years. Considering ultrahigh-energy neutrinos, instruments such as GRAND and IceCube Gen2 Radio, using triggers by the ET+CE network, have a significant probability of detecting at least one coincident GW/neutrino within 15 years [2407].

While such a joint detection can be very informative about the physical processes happening in extreme conditions, it will also improve the sky localisation of the event by orders of magnitude compared to the localisation with GWs only. Considering the huge data we will receive daily with ET, identifying neutrino counterparts for GW events before triggering EM follow-up searches will allow us to improve GW event localisation by identifying joint best-fit GW + ν source location. This will enable us to schedule EM follow-up search initiatives more efficiently, using telescopes with narrow fields of view. All these prospects motivate us to question further the probability of finding a common source of GW and HEN in the era of ET.

5.5 Multi-messenger infrastructure challenges

The large number of alerts generated by ET during both the inspiral phase and the merger of compact objects in binary systems poses significant computational, organizational and logistical challenges. There is a need for dynamic databases capable of efficiently managing a high number of candidate events and the flow of updated information for each of them to send to the astronomical community. These systems must also be able to automatically prioritize events to be characterized with precise parameter estimation. Additionally, ET will

JCAP03(2026)081

need to operate as an EM trigger listener, requiring infrastructure also capable of receiving and processing a large number of external alerts detected by the EM observatories, in order to search for potential temporal and spatial coincidences with GW signals.

The search for gravitational wave signals will not rely solely on the match filtering technique but will also incorporate innovative methodologies aimed also at identifying new classes of signals (see section 8). In this context, advanced multi-messenger analyses that simultaneously integrate spatial and temporal information will be extremely valuable to optimize the identification, characterization, and interpretation of gravitational wave signals.

Multi-messenger astronomy presents critical challenges in terms of interoperability and the application of FAIR (Findable, Accessible, Interoperable, and Reusable) principles. The rapid exchange of information is enabled by the development and adoption of shared standards, facilitating seamless integration and data sharing across heterogeneous research infrastructures. The standardization of processes will be fundamental to allowing scientists to efficiently work with more and more complex datasets from diverse observational sources, including gravitational waves, neutrinos, and traditional electromagnetic signals.

Founded in 2002, the International Virtual Observatory Alliance (IVOA) is a freely accessible consortium that brings together scientific communities, research institutions, and software developers. It functions as an active community and a collaborative forum where members define and discuss protocols for the management, exchange, and analysis of astronomical data. The IVOA protocols currently used by the scientific community for transient events provide a valuable basis for advancing the handling of data and computational demands on a much larger scale. LSST, with its live stream of millions of transients detected every night, will define the protocols and standards for decades to come. A key element of the ET integration in mainstream of multi-messenger astronomy will be the implementation and adoption of open and shared standards, essential for ensuring interoperability across different observational platforms and facilitating data integration and analysis. The use of common protocols will help overcome technological barriers, optimizing the exchange of information among the various components of the multi-messenger network and enabling an effective response to fundamental scientific questions that only a truly integrated approach can address. The ET GW community is collaborating with the EM communities to include the peculiarities of gravitational transients in the upcoming standards and infrastructures.

This section of the paper shows how the realization of ET's full multi-messenger potential will depend on the coordinated development of electromagnetic observational capabilities. Here, we highlight that to maximize scientific return of next-generations multi-messenger observatories, it will also be critical to develop infrastructures, protocol and standards in close coordination.

5.6 Executive Summary

Einstein Telescope will, each year, identify thousands of gravitational wave signals from sources that also emit electromagnetic light. This rich stream of data will provide the opportunity to build the first substantial samples of multi-messenger events. In turn, these objects will enable transformative science across many of the core areas of ET science.

JCAP03(2026)081

Discovery of sources with multiple messengers

- ET-alone is capable of localizing a few hundreds of BNS and NSBH mergers with a localization of tens to hundred of square degrees in size. Although these regions may contain thousands of galaxies, they are sufficiently informative for the electromagnetic observatories to discover an electromagnetic counterpart able to pinpoint the GW source on the sky, identify host galaxies and provide measurements of the distance (redshift) to the source.

- There are many plausible electromagnetic signals that a merging compact object binary may create during or after the merger, including high-energy transients such as **gamma-ray bursts (GRBs)**, **multi-wavelength afterglows** seen from the TeV range through X-ray/Optical/NIR to the radio band, and radioactively powered **kilonovae** emitting dominantly in the optical to mid-infrared. In addition to these EM signals which are dealt with in this chapter, ET may also open new science cases with the joint association of GW to high energy neutrino.

- The identification of these sources in the large gravitational wave sky-localizations is not straightforward, and in this chapter we utilize two state of the art approaches to provide self-consistent estimates of event rates and detectability to the current and next generation of electromagnetic observatories for two proposed configurations of the Einstein Telescope (triangle and 2L) and for ET in a network of 3G detectors. These simulations show that, while ET may identify $> 10,000$ compact object mergers that create electromagnetic light, the majority will remain undetectable to near-term electromagnetic facilities. However, tens to hundreds of events per year will be accessible, providing the first opportunity to build substantial **samples of object detected both in gravitational waves and electromagnetic light**.

Enabling new science

Knowledge of the precise source locations offers a route to addressing a wealth of astrophysical questions, many of which are described in other chapters of this book. In particular, these observations will enable ET data, in concert with electromagnetic observations to:

- Determine the contribution of compact object mergers to **heavy element enrichment** via studies of their kilonovae.

- Study the launching, collimation and emission processes of **relativistic jets** from the post-merger remnant.

- Use the properties of the associated electromagnetic signals to probe the **equation of state of matter at nuclear densities** (see section 7).

JCAP03(2026)081

- Combine electromagnetically determined redshifts with gravitational wave measured distances to measure key **cosmological parameters** (see section 3).
- Use source locations and the demographics of the galaxies which host them to inform the **evolution of the stellar populations** that create compact object binaries (see section 4).

A new paradigm for multi-messenger astronomy

Focus in the current era has been on identifying multi-messenger signals in the relatively nearby Universe. In contrast, the cosmological reach of ET will identify them across cosmic time. This dramatically changes the most likely electromagnetic counterparts and the associated search techniques.

- Our simulations suggest that the best route to growing the multi-messenger samples in the ET era will arise via the detection of coincident gamma-ray burst (or associated high-energy transient) signals. **Realising the scientific return of ET will critically rely on the availability of high-energy instrumentation with good localisation capabilities.**
- **Future observational facilities** will play a crucial role in identifying and characterizing EM counterparts. Photometric (e.g Vera Rubin) and spectroscopic (e.g. WST) instruments will be pivotal for detecting KNe up to $z \sim 0.5$ while large ground and space based telescopes (e.g. ELT, JWST) will be essential for spectroscopic characterization.
- **Radio and X-ray** follow-up will be critical for detecting off-axis afterglows with facilities such as SKA, ngVLA, NewAthena and THESEUS. GW with on-axis GRB counterparts, detected up $z > 2$, will provide valuable insights into the cosmic star formation history of double compact systems.
- The capability of ET to provide several minutes of advanced warning prior to a given merger raises the prospect of sensitive (but still wide field) electromagnetic observations observing the merger in real-time. This opens new EM observational windows for studying **precursor emission, kilonova shock physics and VHE counterparts**. The latter could be efficiently detected by CTAO and other next-generation gamma-ray observatories.
- The identification of EM-signals (e.g. gamma-ray bursts) may be crucial as a route of identifying the GW signals of events of particular interest within the ET data flow.
- **High-energy neutrino observatories** such as IceCube-Gen2, KM3NeT, and Baikal-GVD will play a key role in the multi-messenger network, enhancing the probability of detecting coincident GW–neutrino–EM events.

JCAP03(2026)081

6 Synergies of ET with other gravitational-wave observatories

This section aims to explore the scientific synergies that arise from combining gravitational waves detected by ET with those from other GW observatories. Synergies with other ground based detectors operating between a few Hz and a few kHz, such as the Cosmic Explorer, are crucial for consolidating the science case of ET [15, 16, 1699, 1714]. Synergies with GW observatories at frequencies that are not accessible from Earth-based detectors ($\lesssim$ Hz) broaden instead the scientific reach of ET, allowing for connections to be drawn with different GW sources. This chapter investigates key themes that highlight the scientific advances that are most impactful for the science of ET. The consequences of these synergetic observations span astrophysics, fundamental physics, nuclear physics, late-Universe cosmography, and early-Universe cosmology, offering immense potential for breakthroughs across these fields.

6.1 Introduction

The synergies of ET with other GW observatories enable a *deeper, sharper, and wider* exploration of our Universe, enhancing our understanding of the physical laws that govern it. In certain areas, ET can benefit from complementary observations by other GW observatories, while in others it can uniquely contribute to them, thanks to its high sensitivity and extended observational horizon, especially in the lower range of the high-frequency spectrum around a few Hz.

With ET operating as part of a network of other third-generation (3G) ground-based observatories, such as the Cosmic Explorer (CE) [14], the accuracy of measurements for physical parameters, luminosity distance, and sky localization of GW sources will improve significantly [16, 107, 1167]. The scientific advantages include enhanced cumulative sensitivity, longer observation periods and duty cycles, an extended reach to distant sources, and larger sample sizes of detected events. The baseline configuration considered here includes ET (in either a triangular or 2L configuration) alongside two CE detectors, covering a frequency range from approximately 3 Hz to the kHz region. We will also consider a 3G network made by ET (either in the triangular or in the 2L configuration) together with a single 40 km CE detectors in the US and a LIGO-India detector. In the "high-frequency" range, we also highlight synergies with the proposed Neutron Star Extreme Matter Observatory (NEMO) [2408], a GW interferometer optimized for studying nuclear physics at frequencies above a kHz.

At lower frequencies, we consider different GW observatories in space: the Laser Interferometer Space Antenna (LISA) [330], recently adopted as a flagship mission by ESA in collaboration with NASA, and the concept designs Tian Qin [2409] and Taiji [2410], all of which are sensitive to GWs from below 10^{-4} Hz to about 0.1 Hz. In the decihertz band, we consider the Lunar Gravitational Wave Antenna (LGWA) [2411, 2412] as an example of Moon-based projects (see also LILA; [2413]) and the proposed space mission DECIGO [1952, 2414–2416], with sensitivities extending from about 0.01 Hz up to Hz frequencies. Finally, at even lower frequencies, around the nHz band, we will discuss possible synergies with Pulsar Timing Array (PTA) experiments, using expected radio observations from the Square Kilometre Array (SKA) [2417] as a primary example of a radio telescope infrastructure of interest for our considerations.

JCAP03(2026)081

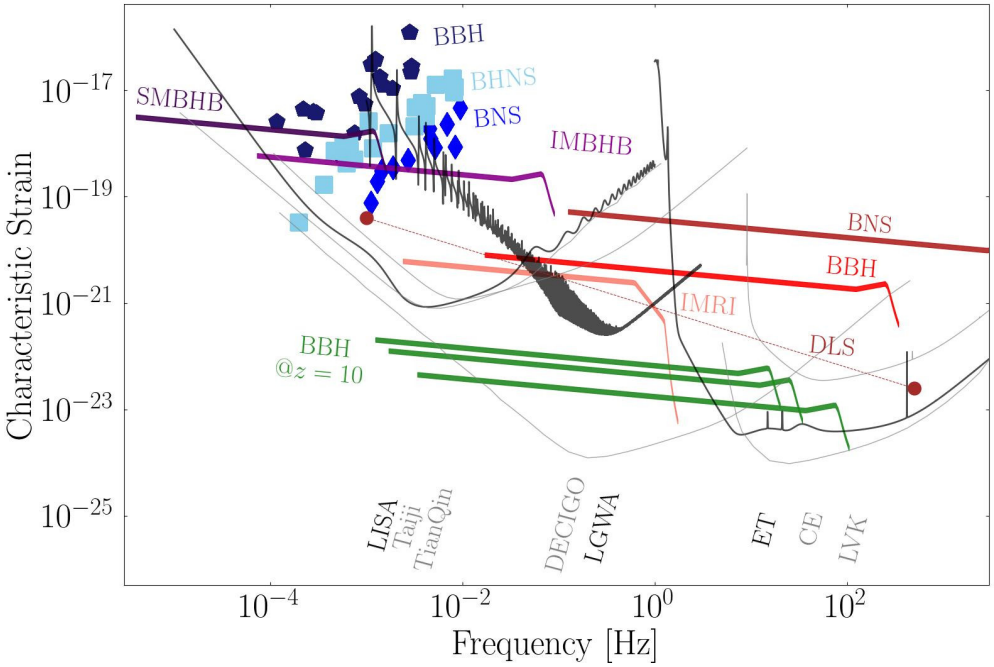

Figure 104. The GW landscape — a schematic representation of synergetic sources in the GW frequency-amplitude plane. The figure shows the sensitivities for ET and CE (including the current LVK detectors) at higher frequencies, and for LISA, Taiji, Tian Qin, DECIGO and LGWA at lower frequencies (sensitivities for the latter are from [330, 2412, 2414, 2416, 2432, 2433]). Tracks (left to right) represent: an equal mass black hole binary merger (labelled SMBH) of $10^6\,M_\odot$ at $z \sim 6$; an equal-mass intermediate mass black hole merger (IMBHB) of $10^5 M_\odot$ at $z = 1.5$; a multi-band source hosting an inspiralling equal-mass stellar black hole binary (BBH) of $60 M_\odot$ at $z \sim 0.1$ merging in the ET bandwidth; an intermediate mass ratio inspiral (IMRI) hosting a stellar black of $30\,M_\odot$ orbiting around a black hole of $5 \times 10^3\,M_\odot$ at $z = 1$. The "BBH@z=10" track denote mergers at $z = 10$ of equal-mass black hole binaries forming in metal poor early galaxies, with a total mass, from bottom to top, of 20, 60, $100\,M_\odot$. Squares, pentagons and diamonds refer to Galactic compact binaries detected by LISA, millions to billions of years away from merging. DLS indicates a dual line system. Each section of this chapter presents each of these sources and their scientific opportunities in detail.

Although we may mention other GW observatories that have been proposed in the literature (e.g. [131, 2418–2431]), at the present stage of developments the ones mentioned above represent the current standard for expected detection capabilities across different frequency ranges during the observational epoch of ET. We will therefore consider these as primary examples providing synergetic observations for ET. In figure 104, we show the sensitivities of some of the GW observatories mentioned above, along with the frequency tracks of few example GW sources.

In section 6.2 we quantify the scientific gains from combining observations of merging binary neutron star (BNS) systems and stellar-mass binary black holes (BBHs) from a network of 3G Earth-based observatories, including ET. These joint observations will deepen our understanding of the properties and evolution of BNSs and stellar-mass BBHs across cosmic epochs and will provide insights into the equation of state of nuclear matter, the dynamics of the Universe on large scales, and the possible existence of exotic compact objects. While

JCAP03(2026)081

these scientific topics are covered in later sections, section 6.2 will focus on the improvements in detection and parameter estimation for these sources. The synergy of combining GW observations of compact binary mergers, such as BNSs and BBHs, can extend to observatories operating at frequencies below a few Hz, which are inaccessible to ground-based observatories. Section 6.2 also discusses nearby extragalactic stellar-mass BBHs, which serve as intrinsic *multi-band GW sources*. When far from coalescence, they emit GWs at frequencies twice their Keplerian orbital frequency, appearing as slowly chirping signals. These low-frequency signals contain unique information about their formation pathways, which is otherwise inaccessible. Detectors such as LISA, Tian Qin, and Taiji can capture these signals at frequencies as low as mHz, long before they enter the Deci-Hz band and eventually merge within ET's frequency range (above a few Hz). Deci-Hz detectors like LGWA and DECIGO will not only track the inspiral of stellar BBHs closely but also observe BNS inspirals, providing early estimates of their masses, distances, and sky locations. These early estimates will allow electromagnetic (EM) telescopes to target these sources long before merger, greatly improving the potential for EM follow-up observations and hence, significantly advancing multi-messenger science.

In section 6.3 we review the expected insights into nuclear physics. The combined measurements of a 3G network of Earth-based observatories will allow for unprecedented constraints on the tidal deformability parameters of NSs and in turn on the state and properties of nuclear matter at extreme densities. These scientific breakthroughs will complement those from nuclear physics experiments at lower energy as well as those from particle physics experiments at higher energy, yielding a complete panorama of the behavior of nuclear matter at all energy scales.

In section 6.4 we present the implications for fundamental physics obtained by the combination of ET with other GW observations. BHs are scale-invariant, vacuum solutions of Einstein's field equations. Probing the spacetime geometry of BHs, i.e. whether they are described by the Kerr metric or not, from the stellar-mass scale to the supermassive scale, is of paramount importance. The benefit of combining ET with CE or with LISA has far reaching consequences. Tests of the nature of black hole horizons, of the orbital evolution during the inspiral phase and of the propagation properties of GWs can be carried out at better precision, given the wider dynamic range that becomes accessible.

The synergy among different GW observatories has the potential to revolutionize late-time cosmology, as discussed in section 6.5. With ET operating as part of a 3G network, the larger dataset, and significantly improved sky localization, will enable better identification of the host galaxies of sources through the detection of EM counterparts of BNS and NSBH systems. These events will serve as unique cosmic tracers, allowing precise measurements of the Universe's expansion, delivering stringent constraints on the Hubble constant, and enabling new tests of the nature of dark energy. Even in the absence of an EM counterpart, the ET+CE network will provide accurate measurements of source masses, sky locations, and distances to enable powerful cosmological analyses. These include measuring the Hubble constant with dark sirens, cross-correlating localization data with galaxy catalogues and exploiting features in the mass distribution of black holes (BHs) and neutron stars (NSs). The large number and extended distance reach of detected GW sources will facilitate precise measurements of the Universe on large scales, offering new insights into current cosmological enigmas and serving as valuable probes at high redshifts.

JCAP03(2026)081

Section 6.6 discusses an additional, albeit indirect, intersection of ET with LISA. This connection addresses an unresolved problem in astrophysics: the origin of supermassive black holes (SMBHs), which range from millions to billions of solar masses and reside at the centres of bright galaxies in the present-day Universe. The discovery of quasars near and beyond the epoch of cosmic reionization raises significant questions about the rapid growth of these massive, accreting black holes. One hypothesis is that these SMBHs form from *seed black holes* of about $10^2\,M_\odot$ to $10^5\,M_\odot$, and grow by accretion and mergers. Among these, light seeds — those lighter than about $10^3 M_\odot$ — are expected to be the relics of the first forming, metal-free massive stars present in the earliest dark matter halos assembling around $z \sim 20$, when the Universe was only a few hundreds of millions of years old. Observing the merger signals of black holes from this first pristine population of stars with ET would establish a connection with the population of merging massive black holes that LISA will detect at comparable and lower redshifts in the mass range around $(10^4 - 10^7)\,M_\odot$. Matching these two independent observations will provide invaluable clues into the physical origin of the seeds, their masses and the processes through which they grew to become supermassive during galaxy evolution. This connection is unique and is made possible since both ET and LISA have comparable cosmic horizon-reaches.

Section 6.7 explores potential synergies between ET, LISA and PTA in the detection of a stochastic GW background (SGWB) from the early Universe (see in particular section 3.2 for discussion of cosmological backgrounds and section 4.10 for discussion of astrophysical backgrounds). By combining these independent observations we can cover a much broader range of GW frequencies and achieve a precise characterization of the expected cosmological background(s). The detailed morphology of the SGWB encapsulates information about the mechanisms that originated the emission of GWs in the early Universe. Complementary observations at different frequencies will thus greatly enhance our ability to precisely characterise these early-Universe phenomena that have produced the detected SGWB. Additionally, the synergy with other Earth-based detectors is crucial for cross-correlating the data of ET and differentiating between noise and stochastic signal. A single interferometer alone will struggle to extract more than an upper bound on SGWBs from the observed data.

In each of the following sections, readers will find two boxes highlighting important text. Cyan boxes outline the main scientific questions associated to the section, while teal boxes summarize key take-home messages of the section.

6.2 Compact object binaries

The stellar-mass compact object binaries in the Universe

- What scientific questions on the astrophysics of neutron stars and black hole binary systems can only be answered with ET in synergy with a network of next generation ground-based observatories?
- What is the promise of multi-band GW observations for understanding compact object binaries?
- Are there dual-frequency GW sources and how will they inform us about the physics of compact objects?

JCAP03(2026)081

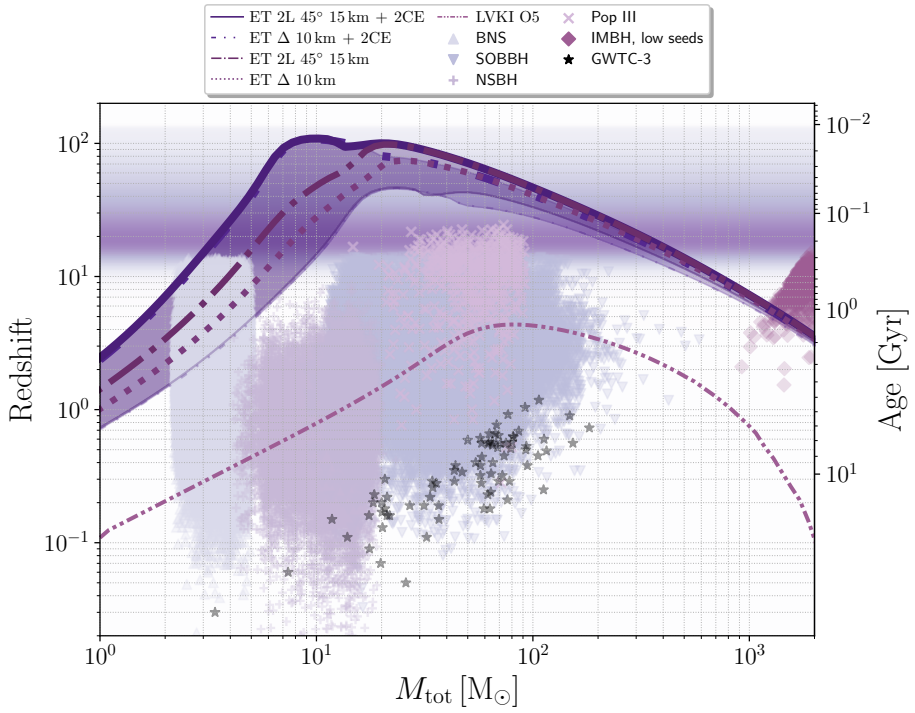

Figure 105. Detector horizons for the two baseline configurations of ET, alone and in conjunction with a network of two CE as described in the legend. The shaded bands, reported only for the combinations with CE, denote the range within which 50% of the sources are detected, when averaging over sky location. Known classes of target sources are reported for illustration: stellar-mass black holes (SOBBH) and double neutron star systems (catalogs from [16]), neutron star-black hole binaries (catalogs from [1167] based on [1370, 1374, 2434]), Population III stars [1674, 1675], and intermediate mass black holes (IMBH) [330]. The orange band is representative of a population of high-redshift primordial black holes (PBHs) [1182, 1738]. Triangles show the events detected by the LVK collaboration [6].

The majority of ET sources will consist of two stellar-mass compact objects with masses in the range $\sim$ 1–1000 $M_\odot$. ET is expected to detect hundreds of thousands of these sources throughout the Universe each year [107, 1167, 1586]. The properties and origin of the population of compact object binaries have only started to be explored, with many formation pathways suggested (see section 4). There is no doubt that ET on its own will enable very significant advances in our understanding of the population and origin of compact object binaries. However, in synergy with other GW detectors, several additional science results are expected, which are highlighted here. We discuss both synergy with high-frequency detectors and with mid-frequency detectors.

6.2.1 Synergy with ground-based detectors

There are several other detectors in the frequency range of ET, from a few Hz to a few kHz, that could provide synergy with ET. The most important one is Cosmic Explorer (CE) [14], a US project for a third generation detector. Einstein Telescope and Cosmic Explorer strengthen and complement each other in important ways. An important difference is that

JCAP03(2026)081

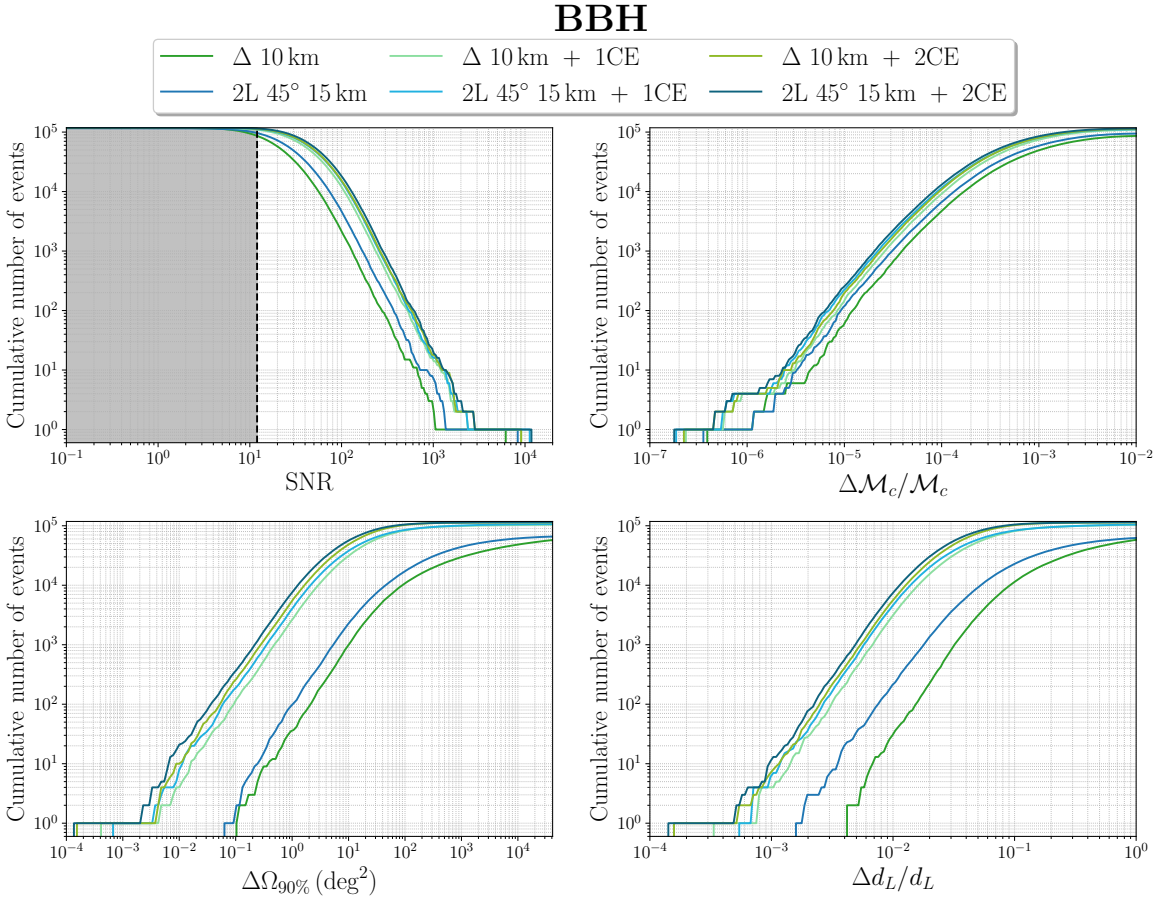

Figure 106. Comparison of SNR and parameter estimation error for the chirp mass, angular localization and luminosity distance for BBHs. We show the results for ET alone, for ET +1CE and for ET+2CE and, in all cases, for ET we consider both the triangle 10 km and the 2L-45° configurations. The results are obtained with the `GWfast` code [2349]; technical details as in [16]. Reproduced from [16]. The Author(s). CC BY 4.0.

CE is expected to be slightly more sensitive in the 10–100 Hz range which will complement the ET sensitivity curve [14], whereas ET is expected to have better sensitivity compared to CE at lower frequencies as a result from ET's underground location that suppresses seismic disturbances, reducing the Newtonian noise that limits CE at low frequencies. To highlight this synergy, figure 105 shows the detection horizons for equal-mass, non-spinning binaries, with a network SNR ≥ 8, for ET in its triangular and 2L configurations, both alone and in a network of two CE detectors.

From just a point of view of detection, ET alone is expected to detect more than 90% of BBHs of stellar origin (SOBBHs) and about 26%(15%) of the binary neutron stars in the 2L (triangular) configuration [16]. This corresponds to $\mathcal{O}(10^5)$ BBH and BNSs detected per year. ET and CE operating in network will allow us to significantly improve range and number of BNS detections. In the ET2L+2CE configuration, the number of BNS sources detectable per year will be $> 4 \times 10^5$ (in the population model considered). Moreover, a network of next generation GW observatories with both ET and CE is crucial to provide orders-of-magnitude

JCAP03(2026)081

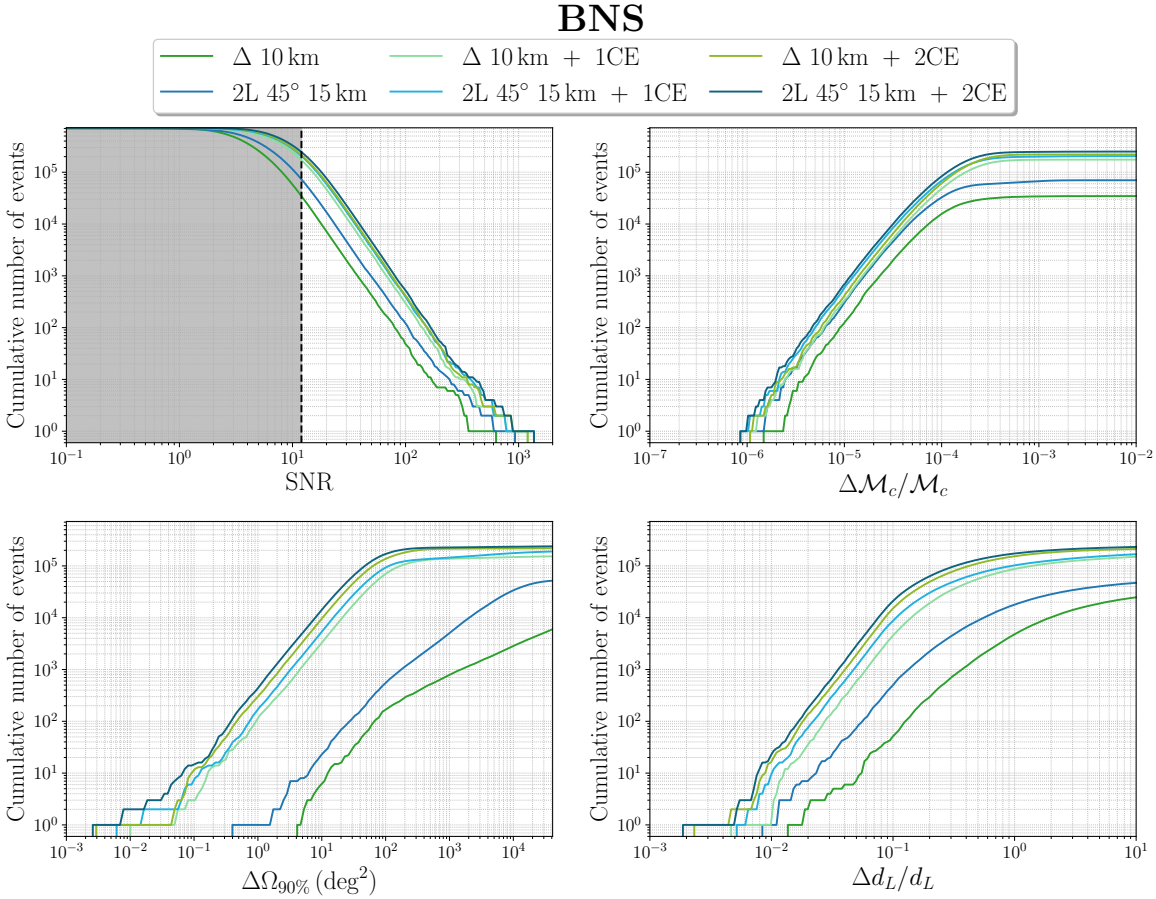

Figure 107. As in figure 106, for BNSs. Reproduced from [16]. The Author(s). CC BY 4.0.

improvement in parameter estimation for coalescing binaries, with significant impact on most of the science goals outlined in the ET and CE studies. As an example, figure 106 shows the SNR distribution as well as the parameter estimation error for the chirp mass, the angular localization and the luminosity distance for the BBHs mergers corresponding to one year of data (using the same population as in [16]), while figure 106 shows the same results for BNS. In both plots we show the results for ET alone, for ET together with a 40 km CE (labeled ET+1CE) and for ET together with a 20 km and a 40 km CE (ET+2CE). In all cases, for ET we consider both the 10 km triangle and the configuration with 2L of 15km at a relative angle of 45°. We see that the improvement is particularly remarkable for angular localization and for luminosity distance (while the improvement in the accuracy of the mass measurement is less dramatic).

Examples of scientific results that can only be found by the combination of ET and CE are: (i) detections of BBHs (BNSs) with 90%-credible sky area less than 0.01 (0.1) deg^2, important for multi-messenger observations [16, 107, 1167]; (ii) regular detection of BNS (BBH) systems at $z > 1$ ($z > 10$) with mass uncertainty $\delta m_1/m_1 < 0.3(0.2)$ [107], important for understanding BH and NS properties across cosmic time, probing fundamental physics and performing precision cosmology; (iii) detection (or strong upper limits on the rate of)

JCAP03(2026)081

primordial black hole mergers at $z \gtrsim 25$ with $\delta z/z < 0.2$ and population III binary black holes at $z \gtrsim 10$ with $\delta z/z < 0.1$, which will be crucial to inform BH formation channels [107, 1178]. Importantly, by being located in the USA, CE will provide a longer baseline that will improve sky localizations and parameter estimations [107, 1167, 1586], as we see from figures 106 and 107. Having both CE and ET will also be beneficial for increasing the completeness of the observed population: for example, a network with both ET and CE will achieve 50% completeness of BNS sources up to $z \sim 2$, as can be seen in figure 105, whereas an (A+)-like network will only achieve that for $z \sim 0.2$ [1586]. Furthermore, having both ET and CE will increase the time that at least one detector is always online to assure measurements are made during exceptional events such as a galactic supernova [107, 1167, 1586].

Overall, the presence of a next-generation detector network, including ET and CE, will enhance the science obtainable from ET observing alone. Fields such as those related to the measurement of cosmological parameters, unraveling the nuclear equation of state, and making new discoveries such as the presence of dark matter around NSs or BHs, multi-messenger merger observations can largely benefit from the improved capabilities of a network of observatories [14, 107, 1167, 1586]. Similar synergies can be outlined between ET and the Neutron Star Extreme Matter Observatory (NEMO) [2408], a proposed GW interferometer optimized to study nuclear physics with merging neutron stars which, together with ET, could contribute to inform the physics of BHs and NSs and their progenitors.

Another network configuration which could be possible in the next-generation era is made of ET (either in its triangular or in its 2L configuration) together with a single 40 km CE detector in the US and LIGO-India. This configuration has been recently studied in [107, 2435] (restricting however to ET in its triangular configuration). LIGO-India, currently under construction in Aundha, India, will feature 4 km arms as its US counterparts and is expected to be operational in the 2030s at A+ sensitivity [392], with upgrades at A$^\#$ sensitivity levels [2436]. As shown in [107, 2435], the results obtained with this network are quite interesting. Indeed, with respect to a network made by ET together with a 40 km CE and a 20 km CE one finds that, for angular localization and accuracy on luminosity distance, replacing the 20 km CE detector with LIGO-India operating at A$^\#$ sensitivity gives nearly identical performances, since the factor of five in arm length is offset by the increase in baseline relative to a second CE (although other aspects of the science case are limited by the shorter arm length and narrower sensitivity band).

Here we perform again the analysis for a network made by ET together with a single 40 km CE detector and LIGO-India, extending the analysis of [2435] by considering both the triangular and the 2L configuration of ET, and assuming A$^\#$ sensitivity for LIGO-India. For uniformity with the results shown in figures 106 and 107, as well as with similar analysis presented elsewhere in this paper (see in particular section 10) we use the same population model, sensitivity curve and technical details as in [16].[54] The results are shown in figures 108

[54]To compare with the results presented for BNS in [2435] one must take into account some technical differences. Our population model, restricting (as in [2435]) to $z < 0.5$, contains 1.1×10^4 BNS (and corresponds to a local merger rate $R_0 = 250\,\mathrm{Gpc^{-3}yr^{-1}}$), to be compared with 1.6×10^4 BNS (and $R_0 = 320\,\mathrm{Gpc^{-3}yr^{-1}}$) in [2435]. Furthermore, we assume an uncorrelated 85% duty cycle in each L-shaped detector, and in each of the three instruments composing the triangle, while [2435] uses 100% for the duty cycle; this affects in particular the number of rare events with the very best accuracy of reconstruction. We have checked that,

JCAP03(2026)081

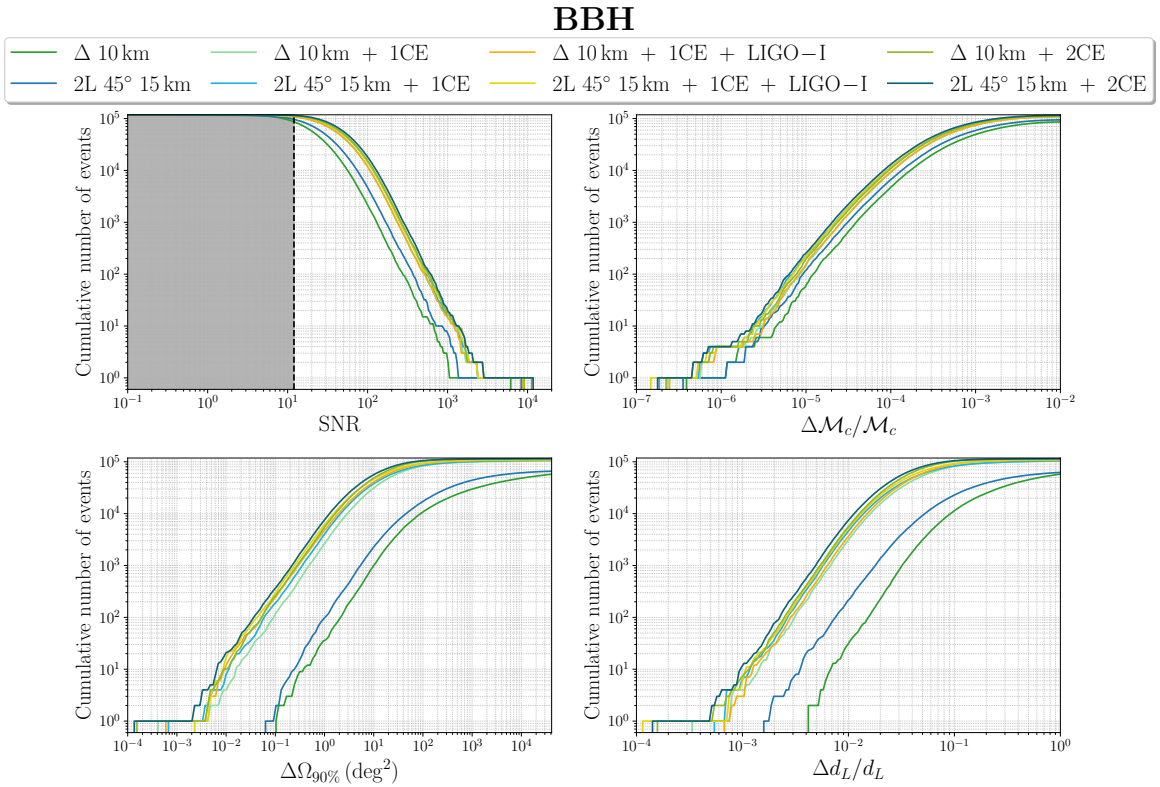

Figure 108. Comparison of SNR and parameter estimation error for the chirp mass, angular localization and luminosity distance for BBHs for different networks (as in the legend), including networks involving LIGO-India. The results are obtained with the `GWfast` code [2349]; technical details as in [16]. Reproduced from [16]. The Author(s). CC BY 4.0.

for BBHs and in figure 109 for BNSs, and show that a network made by ET together with a single 40km CE detector and LIGO-India can be quite competitive.

6.2.2 Synergies with space-borne detectors

The synergies with space-borne detectors, in particular LISA, the space mission recently adopted by ESA in collaboration with NASA [330], and operating in the "mid-frequency" band $\sim 10^{-4} - 10^{-1}$ Hz, come in three distinct ways: i) observations of *different instances* of a class of compact object binaries at lower frequency, that provide complementary insight in their population properties and their origin; ii) observations of *multi-band* sources, that are first observed at mid-frequency and then later in the ET band; and iii) *dual-line sources* that emit simultaneously in both mid-frequency band and the ET band.

Observations of the same source class. Different origins of compact object binaries (from isolated binaries, from dynamical processes, or from primordial black holes) give rise to different population properties that can be used to disentangle their origin, e.g. [2437]. Orbital eccentricity is thought to be a significant indicator of formation via dynamical

if we use 100% duty cycle and take into account the different BNS rate, the results are consistent, within a factor of 2, with those in [2435].

JCAP03(2026)081

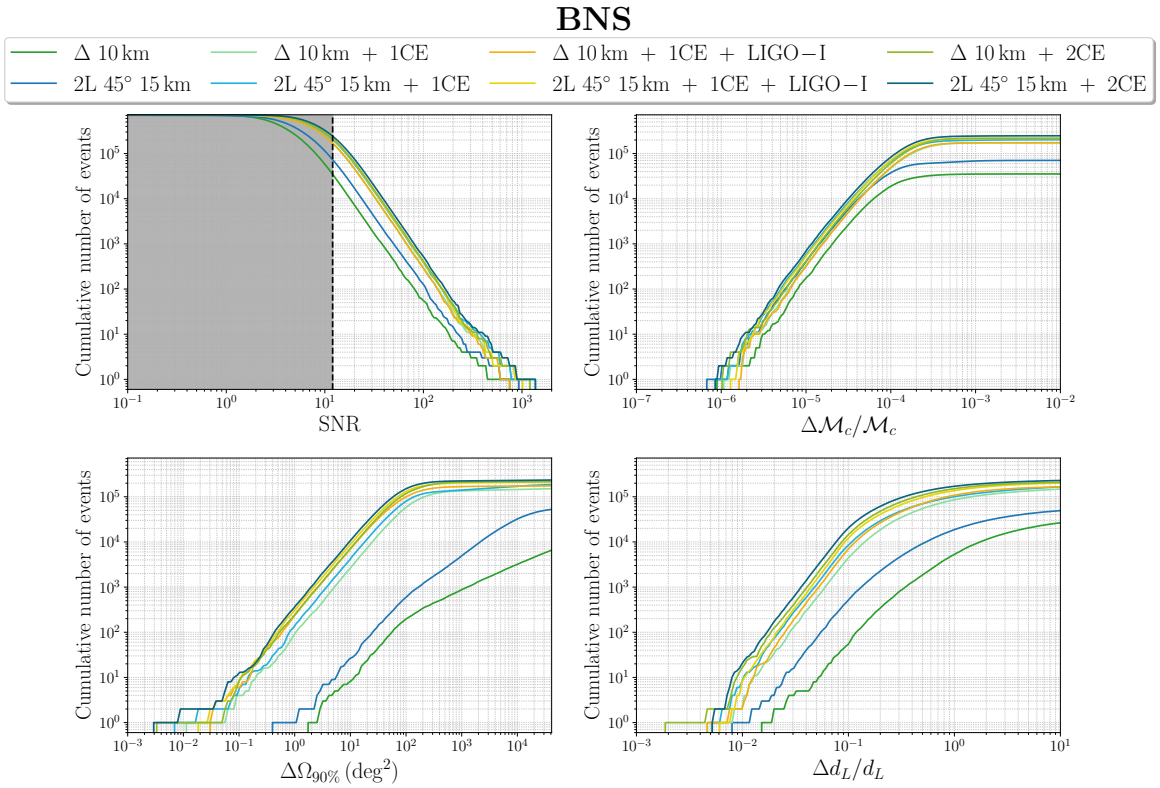

Figure 109. As in figure 108, for BNSs. Reproduced from [16]. The Author(s). CC BY 4.0.

processes and can be detected by LISA, but cannot easily be measured by high-frequency detectors, since the eccentricity is radiated away by GW and it very small by the time the signals enter the detectable band, even for large initial eccentricity [1521, 2437]. Observing the same type of sources at much lower frequency is an excellent way to constrain the importance of dynamical formation, albeit only in the nearby Universe, since LISA and similar detectors typically observe stellar-mass binary black holes in the Milky Way and nearby galaxies [2438], unless they are at very high frequency when they can be observed to several tens or at most hundreds of Mpc, see [512]. Deci-Hz observatories such as DECIGO would in fact be even better at detecting eccentricity given the large number of sources they can observe up to cosmological distances [1458].

Multi-band sources. These are binary black holes that are observed in the LISA band and then later, on human time scales (years), merge in the high-frequency band [2439]. In order for this to happen the binaries must have heavy black holes of around 30 $M_\odot$ or higher. Such heavy sources have been observed already with the current detectors. However, the expected number of multi-band systems that will be observed with LISA is likely small [2440, 2441]. The scientific value of these measurements would be high: the LISA measurements can make a very accurate prediction of the time and sky localisation of the merger in the ET band and the properties of these systems would be determined to very high accuracy, see e.g. [2442]. Another proposed special class of multi-band sources is a low-frequency binary black hole orbiting around a super-massive black hole, where high induced eccentricity could move the

JCAP03(2026)081

system temporarily into the ET band [2443]. Multi-band sources would as well be ideal targets for Deci-Hz detectors, as these observatories will be able to closely follow their inspiral almost until the merger, providing a strong complementarity with ET measurements and excellent pre-localisation accuracy for multi-messenger studies [2412, 2444–2447].

Dual-line sources. These are proposed sources emitting simultaneously in two frequency bands. An example are ultra-compact X-ray binaries consisting of a rapidly rotating NS (with spin frequencies in the hundreds of Hz) orbiting a companion star [1897]. GW from the orbital motion can be detected by LISA while continuous GWs can be detected in the ET band due to the presence of accretion-built mountains, toroidal magnetic fields, and/or r-mode oscillations [1898]. A dual-line detection could provide percent-level constraints on the mass, radius, and internal magnetic field strength of the neutron star. With ET, at least four of the known ultra-compact binaries become potentially dual-line detectable [1898].

6.2.3 Stochastic background from compact binaries

Finally, there is added value in correlating GW observations between different instruments for the detection of broadband stochastic signals that make up the astrophysical GW background, e.g. [100, 2448] to both characterize the population of astrophysical GW sources and distinguish these from cosmological backgrounds, as discussed in section 10.5.3. In the ET frequency band, the astrophysical GW background is the collective signal produced by unresolved black hole and neutron star binaries, and can be detected by ET with significant confidence (see section 4.10). However, its broadband features imply it may be difficult to distinguish from instrumental noise, particularly when the latter is not very well known, see e.g. [540]. Cross-correlating measurements of different, independent instruments, such as ET and CE will thus increase detection confidence.

In addition, there is synergy with detection efforts in other frequency bands: the same binary background extends to lower frequencies and can in principle be detected by detectors such as LISA and Tian Qin. A multi-band detection and characterization effort would provide additional constraints on compact binary population features, including information on compact binary progenitors, see e.g. [2205, 2211, 2212, 2449], complementary to those coming from resolved source analyses. Furthermore, low frequencies such as those monitored by LISA will be dominated by a broadband stochastic foreground due to unresolved white dwarf binaries (that, due to the relatively large size of the white dwarfs, does not contribute to the ground-based detector GW band). Recent studies suggest that the white dwarf background may well dominate LISA data, hindering detection prospects for the stellar-mass compact object background [2450, 2451]. In this scenario, detection of this background signal with ET will be all the more valuable, and will be used to inform analyses at lower frequencies.

A notable data analysis challenge in this context will be component separation. Differentiating between resolved events and background and between background contributions of various nature requires novel analysis techniques, and in particular the residual subtraction error could dominate stochastic measurements [2452, 2453]. However, recent work that performed explicitly the correlation between data streams of different detectors, after reconstruction and subtraction of CBCs from the individual detector data streams, show that the enhanced resolving power of a network made of ET+CE can reduce significantly the errors

JCAP03(2026)081

in the reconstruction of resolved sources, to the extent that the sensitivity to cosmological stochastic background will only be marginally affected, see [643] and section 10.5.3.

Take Home Message

- ET in a 3G network alongside other ground-based detectors, such as Cosmic Explorer, will extend the cosmic horizon reach, enable deeper and more accurate surveys, and yield significantly more precise physical measurements of stellar-mass compact object binaries.
- Joint observations with a ground-based GW network (ET with CE or NEMO) will enable us to map neutron stars across cosmic time.
- Synergies between ET and lower-frequency space-based detectors, such as LISA, will enable multi-band observations of the same source classes, offering unique insights into their formation pathways.
- Multi-band observations of the same source are essential to discover dual-line.
- Astrophysical, stochastic GW signals from compact binaries of diverse type and in different evolutionary states are expected to be detected by ET and LISA. These observations will provide unique statistical information into the underlying source populations.

6.3 Nuclear physics

Nuclear Physics in the Realm of GW Sources

- How many more BNS and NSBH mergers we can observe with ET+CE? How does it translate to constraints on EoS?
- How much better can we observe the post-merger phase of a BNS merger? How does it translate to QCD phase transition constraint?

A principal goal of heavy-ion collision experiments such as Relativistic Heavy Ion Collisions (RHIC) [2454] and Facility for Rare Isotope Beams (FRIB) [2455] is to understand the nature of hot and dense hadronic matter. These experiments have improved our understanding of the quark-gluon plasma, a state of matter thought to have existed in the early moments after the Big Bang. However, much about the properties of this matter remains unknown. At the other end of the spectrum, neutron star cores are believed to contain matter at even higher densities, though at much colder temperatures than those explored in heavy-ion collision experiments.

During the inspiral phase of a neutron star merger, the properties of the cold supranuclear matter are encoded in the tidal dephasing of the signal. The supranuclear matter can reach a temperature of 50 MeV [2456–2458] during the post-merger phase. Therefore, the observation of a binary neutron star merger provides a unique opportunity to explore the QCD phase

JCAP03(2026)081

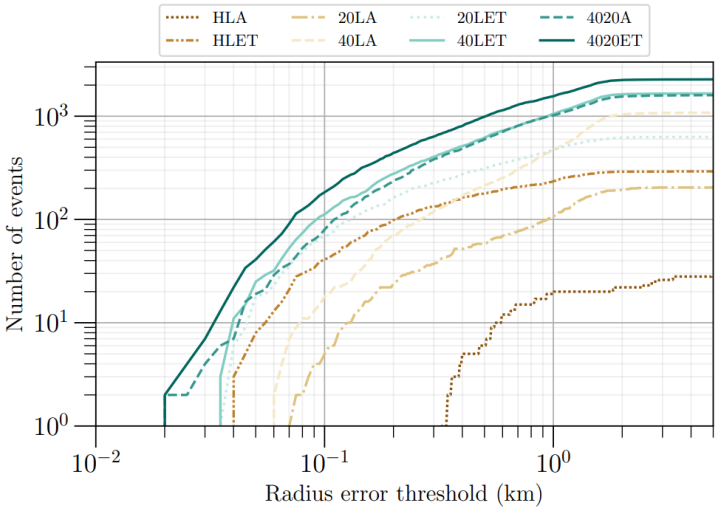

Figure 110. The cumulative number of GW detections (vertical axis) for which it will be possible to constrain NS radii below a specified threshold (horizontal axis) is shown. The lines represent different GW detector configurations: HLET, 20LA, and 40LA indicate networks with one next-generation detector, while 4020A, 20LET, and 40LET represent networks with two next-generation observatories. Figure reproduced with permission from [107].

diagram comprehensively, spanning both cold and hot regimes of dense matter, as we discuss in detail in section 7.

In this section, we showcase how the synergy between ET and CE can: (1) constrain the cold supranuclear matter with the thousands of neutron star merger detections; (2) detect the currently undetectable post-merger signal; (3) gain insights about the supranuclear matter with the post-merger signal.

6.3.1 Population approaches for nuclear physics

Next-generation GW observatories will detect thousands of binary coalescences involving a neutron star (NS) [16, 107]. These mergers are rich laboratories to study the behavior of matter under extreme conditions [2459], as also demonstrated by the binary neutron star GW170817 [4, 2288]. When the NS approaches its companion, in particular a BH, it may undergo tidal deformation and be disrupted. This process imprints a distinctive signature on the GW waveform that is parametrized with a tidal deformation parameter Λ for the NS (see eqs. (7.4) and (7.5) below). From the knowledge of Λ and the NS mass, it becomes possible to estimate the NS radius. Finally, a joint estimation of the NS mass and radius is crucial for determining the Equation of State (EoS) that governs the star mass-radius relation [2460]. However, the EOS for neutron stars remains unknown and measuring NS radii is extremely challenging as the Λ parameters are not often well constrained. The BNS merger GW170817 currently provides the best constraint on the NS radii, with a precision of a few kilometres [2460]. This precision was only sufficient to exclude the stiffest EoSs.

Next-generation observatories will detect thousands of GW events like GW170817, including hundreds of sources with higher signal-to-noise ratio [16, 107, 1167]. Figure 110

JCAP03(2026)081

shows the forecasted constraints on the NS radii achievable in the next-generation GW era. For a GW detector network that includes at least one next-generation GW detector, it is anticipated that NS radii can be measured with a precision of 1 km (approximately 10% of the nominal NS radius) for about 200 detections per year [107]. In a network with at least two next-generation GW observatories, this number increases to around 1,000 detections annually. These observations would provide the robust data necessary to precisely test and refine proposed EoSs for NSs [1231, 1239]. The ability of 3G observatories to constrain the NS EOS from populations of compact binary coalescences is not significantly affected by the specific geometries of the detectors but rather depends on the number of 3G observatories available to capture these signals [1231].

6.3.2 Measurability of the post-merger phase signal

The post-merger phase explores a different regime in the QCD phase diagram, characterized by significantly higher densities and temperatures compared to the inspiral phase. During the inspiral, the neutron stars remain largely intact, and the densities reached are limited to their central densities, approximately 3–4 times the nuclear saturation density. On the other hand, the post-merger phase probes densities exceeding five times nuclear saturation density [2461]. At temperatures of approximately 50 MeV, the effects of different transport coefficients become prominent, leaving noticeable imprints on the data [2456–2458]. However, the amplitude of the post-merger phase signal is weaker than that of the inspiral phase due to the reduced quadrupole component [2462–2466]. This challenge is compounded by the reduced sensitivity of current detectors at the higher frequencies where the post-merger signal lies. However, a next-generation GW detector significantly improves access to the post-merger phase. As shown in table 10, for three sources taken at the same distance of 68 Mpc,[55] but different values of the masses and of the tidal deformability, the post-merger phase SNR is five times higher in the next-generation GW detector network as compared to current generation networks.

To translate the SNR into physically meaningful parameters, parameter inference must be conducted within a next-generation GW detector network. Figure 111 illustrates that including the post-merger phase and linking its parameters to those of the inspiral phase using quasi-universal relations (QU-PM) results in significantly tighter posteriors for tidal deformability compared to analyses that exclude the post-merger phase (NO-PM). This demonstrates the potential of the post-merger phase to enhance studies of cold supranuclear matter. Additionally, as shown in figure 112, the parameters of the post-merger phase are only measurable with a next-generation GW detector network. This highlights the critical role of the post-merger phase in studying hot supranuclear matter, contingent on the availability of a next-generation GW detector network.

A network of next generation GW observatories is essential for breaking degeneracies among waveform parameters. Adding interferometers such as NEMO [2408], which are

[55]This specific value of the distance was chosen in [2467] because, as we see from the row labeled LHV in table 10, in a network made by Advanced LIGO+ and Advanced Virgo+, it corresponds to a signal-to-noise ratio of 100 for Source 1 (which is defined by the masses and tidal deformability given in the table caption).

JCAP03(2026)081

	Source1		Source2		Source3	
	Total	PM	Total	PM	Total	PM
LHV	100	2.0	94	2.5	100	2.7
ET-CE	1267	10.2	1190	12.3	1268	13.3

Table 10. The SNRs for three source located at a distance of 68 Mpc and with chirp mass, mass ratio and tidal deformability as follows. Source 1: $\{\mathcal{M}_c = 1.17524\,M_\odot, q = 0.8, \tilde{\Lambda} = 604\}$; Source 2: $\{\mathcal{M}_c = 1.08819\,M_\odot, q = 1.0, \tilde{\Lambda} = 966\}$; Source 3: $\{\mathcal{M}_c = 1.17524\,M_\odot, q = 1.0, \tilde{\Lambda} = 607\}$. The table includes the SNR for the entire waveform (labeled as "Total") and for the post-merger phase specifically (labeled as "PM"). See ref. [2467] for details. Reprinted figure with permission from [2467], Copyright (2023) by the American Physical Society.

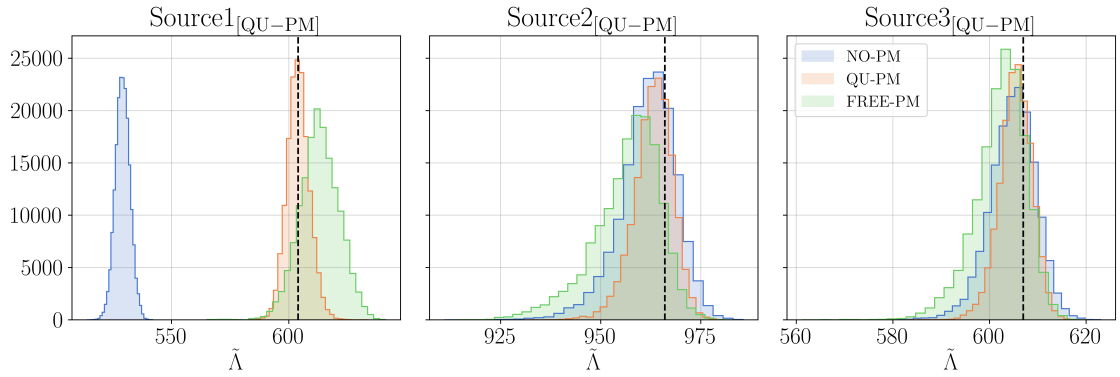

Figure 111. Posterior probability density for $\tilde{\Lambda}$ (see eq. (7.5) for definition) for sources observed by the ET+CE network, recovered with three different models NO-PM (without post-merger phase), QU-PM (with post-merger phase and employing quasi-universal relation), and Free-PM (with post-merger phase and its parameters freed from that of the inspiral phase), in blue, orange, and green, respectively. The black dashed lines correspond to the injected values. The parameters (distance, masses, tidal deformability $\tilde{\Lambda}$) of the three sources are the same as in table 10. Reprinted figure with permission from [2467], Copyright (2023) by the American Physical Society.

optimised for the higher-end of the high-frequency GW spectrum, would provide even stronger constraints on the EoS, thanks to a more precise characterisation of the post-merger phase.

6.3.3 Inferring exotic nuclear phenomena with binary neutron star mergers

The merger of BNS systems can result in a dense NS remnant that can resist gravitational collapse for timescales ranging from several milliseconds to a few minutes after merger [2468, 2469]. The post-merger evolution of these remnants results in GW emission [2470], making them promising candidates for understanding the behavior of matter at extreme densities. These remnants have been shown to potentially exhibit several exotic phenomena, such as phase transitions to deconfined quarks [2471, 2472], deconfined quarks *via* quark-hadron crossover [2473, 2474], formation of absolutely stable strange quark matter [2327, 2475], the appearance of hyperons [2476, 2477], and thermal effects [2478, 2479]; see section 7.3.2.1 for more detailed discussion.

JCAP03(2026)081

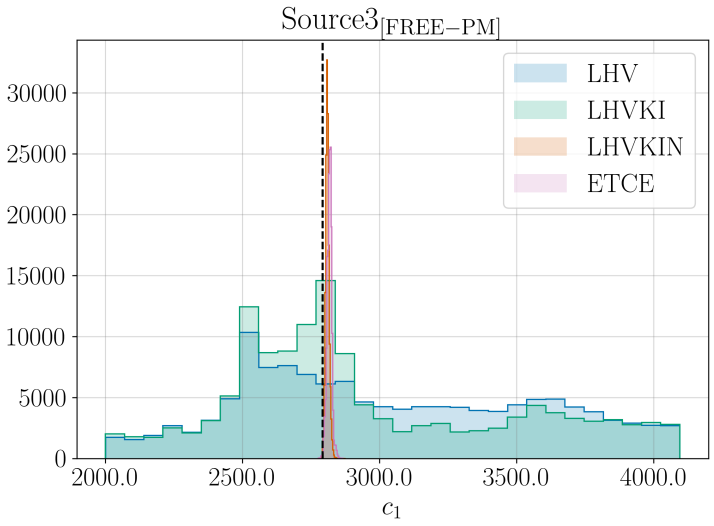

Figure 112. Posterior probability density for c_1, one of the post-merger phase Lorentzian parameter for different detector networks. The dashed vertical line indicates the injected value. Reprinted figure with permission from [2467], Copyright (2023) by the American Physical Society.

Among other outcomes, these effects can alter the compactness of the remnant (compared to the cold hadronic equation of state), thereby affecting the value of the peak post-merger frequency, f_2. Hence, precise measurement of f_2 is important for inferring the nuclear processes occurring within the dense remnant. Ref. [1234] finds that deviations in f_2 caused by phase transitions can be detected with 90% confidence for a post-merger SNR of 10. This corresponds to an inspiral SNR of approximately 600, achievable by ET alone at distances $\sim 90\,\mathrm{Mpc}$. The 20 km CE detector, when optimized towards post-merger frequencies, can accumulate the same post-merger SNR at $\sim 120\,\mathrm{Mpc}$. For the crossover scenario, ref. [2480] employs a Bayesian model selection to claim that a crossover to the quark phase will be detectable with ET and CE observatories for a few BNS mergers every year. Further, the deviation in f_2 due to thermal effects can be detected with 90% credibility for a post-merger SNR of 15, achievable for by ET for events at 50 Mpc [2479]. Together with CE, such events can be detected with the same SNR up to higher distances, which will increase the rate of detection of these events.

While phase transitions to quark matter are expected to affect post-merger signals due to their relevance at high densities, several studies suggest that signatures of strong phase transitions may also appear in the inspiral phase. Single or sequential phase transitions can lead to significant deviations in the mass-radius ($M - R$) relationship compared to their hadronic counterparts [2481, 2482]. EoSs with first-order phase transitions may exhibit small deviations in the tidal deformability parameter Λ while causing variations in the radius on the order $\mathcal{O}(100)$ m [2483]. Detecting such changes due to phase transitions using GWs alone requires precise measurements of both radius and Λ, which can only be achieved with next-generation GW observatories. Using a non-parametric approach, ref. [2484] finds that a catalog of several hundred BNS mergers would be necessary to confidently detect phase

JCAP03(2026)081

transitions, a capability that would only be feasible in the next-generation GW detector era. However, ref. [2485] demonstrates that if the phase transition occurs at twice the nuclear saturation density, it could be confidently inferred from a single BNS event at a distance of $\mathcal{O}(100)$ Mpc with next-generation GW observatories.

Hence, precise measurement of NS parameters in both pre- and post-merger GW signals from BNS mergers will allow the inference of exotic nuclear processes. Such detailed and numerous estimates will only be achievable with a network that includes both ET and CE observatories.

Take home message

The synergies between ET and other Earth-based GW observatories are essential for achieving a comprehensive and robust understanding matter at supranuclear densities.

6.4 Fundamental physics

Stellar- and intermediate-mass BBH systems serve as exceptional laboratories for testing General Relativity (GR). Stellar-mass BBHs evolve over long timescales within the LISA frequency band, where their dynamics can be accurately described using the post-Newtonian (PN) approximation [32]. As they gradually inspiral out of LISA's range and transition into the frequency band of ET, their dynamics enter a highly non-linear regime that eventually necessitates numerical relativity (NR) simulations. Multi-band observations of these systems thus provide a unique avenue to probe both lower-order PN predictions and the strong-field effects captured by NR simulations, offering a comprehensive test of GR across a wide range of physical regimes.

In contrast, intermediate-mass BBH systems have shorter lifespans in both the LISA and ET bands, but their significantly larger signal strains and SNRs enable unique tests of GR. In the LISA band, these systems allow exploration of mildly non-linear dynamics during the inspiral phase, while in the ET band, their post-merger signals probe the strongly non-linear regime. Additionally, concurrent observations by ET and CE will provide an unprecedented opportunity to test the polarization properties of the waves, further advancing our understanding of gravitational phenomena in the strong-field regime. The synergetic fundamental physics exploration with ET are enumerated in the box below.

Synergetic Fundamental Physics

- Multi-band observations of the inspiral, merger and ringdown phases of compact binary coalescences offer a unique opportunity for precision tests of GR.
- Joint observations by ET and CE can help break degeneracies.

As we have discussed in detail in section 2, one of the fundamental science objectives of ET is to test General Relativity (GR). ET alone will be able to test GR to incredible precision with the detection of black hole binaries like GW150914 with an SNR of more than

JCAP03(2026)081

1000. With multi-band observations with space interferometers the precision to which the theory can be tested increases by a order of magnitude. Additionally, combining ET and CE data will help test the theory in new regimes such as polarization states and lensing of the observed gravitational waves as they would require accurate sky pointing and distance measurements. In the reminder of this subsection we discuss how ET can achieve greater sensitivity to test GR with data from other terrestrial and space-based GW observatories.

6.4.1 Tests of the inspiral phase

In GR, the phase evolution of a binary system is driven by a balance equation between the change in orbital energy and the energy flux emitted in GWs. During the inspiral, this evolution is well represented by the post-Newtonian approach [32], that permits to derive a perturbative series for the phase evolution written in terms of the small PN parameter $v = (GM\omega/c^3)^{1/3}$ for a total mass M and orbital frequency ω, with v^2 denoting the PN order parameter. In GR, the dominant term in the phase evolution is driven by the quadrupole radiation and is $\propto v^{-5}$; it is often called Newtonian, or 0PN, term. High and low (or negative) PN orders affect most the late or early inspiral, respectively.

In alternative theories of gravity, this structure can be modified due to either the existence of extra fields or a modification of the gravitational dynamics. One well-known example is dipolar radiation, present generically in theories featuring scalar or vector fields [2486], which appears at leading order at the -1PN order with respect to the quadrupole radiation. Because dipole radiation appears at a relative lower order of -1PN with respect to the quadrupole radiation, it affects most prominently the early inspiral of a binary and represents a valuable window to look for clues of new physics in the gravity sector [2487]

Among proposed modifications from GR (see e.g. table VII in [2488]), time-dependent variations of the gravitational constant itself create a negative -4PN correction; modifications of black hole evaporation in large extra dimensions also yield a -4PN term; scalar-tensor theories such as Jordan-Fierz-Brans-Dicke and Einstein-Dilaton-Gauss-Bonnet theories, as well as Einstein-Aether theories will all feature dipolar radiation with a -1PN leading term; introducing a graviton mass yields a 1PN term; parity-violating Dynamical Chern-Simmons theory and some models of non-commutative gravity will introduce a modification at the 2PN order.

In this landscape, negative PN orders will affect most prominently the early inspiral, while positive PN orders will affect the late inspiral the most. This creates a strong trend across instruments: observations sensitive to the late inspiral and merger of a binary system, such as massive BH binaries (MBHBs) in LISA or stellar-mass BH binaries (SBHBs) in ET, are typically best to constrain high PN orders, while observations sensitive to the early inspiral, such as SBHBs for LISA or binary pulsar timing, are best to constrain negative PN orders. Notably, dipolar radiation might even dominate over the quadrupolar radiation at low enough frequencies. However, if multi-band GW observations are made, the high-frequency band data can also help a lot in inferring parameters that are otherwise degenerate if only low-frequency data are available.

This synergy has been explored in many recent works. Ref. [73] proposed a theory-agnostic test on black-hole dipolar radiation, combining the LISA band and the band of

JCAP03(2026)081

ground-based instruments. Ref. [2489] explored this multi-band synergy for parity-violating gravity, ref. [2490] for parity-violating gravity as well as scalar-tensor theories, ref. [2491] in the form of a theory-agnostic test at every PN order. These studies relied on the Fisher matrix approximation for parameter recovery. Ref. [2492] used Bayesian inference for the LISA data with priors from ground-based instruments to simulate an analysis of dipolar radiation and graviton mass. The emerging view from these studies is clear: multi-band observations would significantly improve over the constraints that could be achieved with LISA or ET alone.

Beyond multi-band observations with LISA, a similarly synergy would exist with instruments in the Deci-Hz band. Ref. [2493] demonstrated that by combining data from ground-based observatories such as ET and CE with data from milli-Hertz observatory (e.g., LISA) or Deci-Hertz observatory (e.g. DECIGO) the parameter precision on the dipolar-radiation parameter indeed improves by several orders of magnitude. Similar improvements were also found [2494] by performing joint parameter estimation using ET and atom-interferometer gravitational-wave observatories that are also investigated for operating in the Deci-Hertz band [2431, 2495].

In cases where dipolar GW radiation happens, it is common to simultaneously have a varying gravitational constant, e.g. in the scalar-tensor theory [2486, 2496]. Ref. [2497] showed that a synergy between ET and other deci-hertz gravitational-wave observatories will be able to simultaneously test the effects from dipolar radiation and a linear-in-time evolving gravitational constant, thus constraining the underlying gravity theory from multiple angles.

A somewhat different scenario has been proposed where multi-band observations would be valuable: in presence of ultralight boson clouds around black holes, a GW detection in the LISA band could direct a search in ET for a continuous wave generated by clouds orbiting the remnant of the merger [2498].

6.4.2 Tests of the merger and ringdown

Multi-band observations with LISA and ET would provide a different view for model-agnostic tests checking the consistency of the signal in its inspiral and merger-ringdown phases, by providing independent information on the inspiral and improving the overall parameter estimation [2499]. This would be particularly important in providing a view of the inspiral of massive systems only detectable at merger in the ET band [2489, 2500].

Multi-band observations also provide an important operational input for ringdown analyses: SBHBs observed by LISA before their merger will be among the loudest targets of ground-based instruments, and an advance warning would allow us to make sure that the ground network will be fully operational and at optimal sensitivity by the time the merger occurs. It is also possible, in principle at least, to tune ground-based interferometers to achieve an increased sensitivity in a narrow frequency band that can be chosen to maximize the precision of ringdown tests for a particular binary, achieving an improvement by a factor of 2 [2501].

6.4.3 Tests of frequency-dependent speed of GWs

A particularly important consequence of the observation of the bright siren event GW170817 has been the determination of the propagation speed of GWs to be the speed of light within

JCAP03(2026)081

10^{-15} [2, 4]. This bound applies to GWs in the frequency range probed by ground-based interferometers. However, in an effective field theory approach to dark energy, the GW frequencies probed by ground-based interferometers lie around the typical strong coupling scale of the EFT, leaving the possibility that an appropriate ultraviolet completion of dark energy scenarios could avoid present constraints on the GW speed, while still showing deviations at lower frequencies [1263, 2502]. Refs. [2502] and [2503] showed however that a single multi-band observation of a GW150914-like event by LISA and a ground-based interferometer would allow to constrain the speed of GWs to match the speed of light within 10^{-15} across a much wider frequency range.

6.4.4 Tests of the GW polarization

In modified theories of gravity, GW signals can typically feature additional modes of polarization beyond the usual transverse-traceless tensor modes $h_+, h_\times$ [2486]. In the most general case, the GW can comprise up to 6 modes, two transverse tensorial modes, two vectorial modes, a breathing scalar mode and a longitudinal scalar mode [72, 2486]. Although the dominant effect of modifications to GR tends to be the contribution to the orbital phasing, and thereby to the phase of tensorial modes, the GW itself will also be modified by the addition of these extra modes of polarization, for instance due to the additional energy loss in dipolar radiation. Since this is in essence an amplitude correction rather than a phase correction, constraints on the parameters of specific modified gravity theories are typically weak. However, checking the tensorial nature of GWs can also be seen as a theory-independent verification of the consistency of GR with the data, and different polarization hypotheses can be compared using null-stream methods [8, 96].

Because each detector (or TDI channel in the LISA case) is only sensitive at any given time to a projection of the gravitational wave, constraining additional modes of polarization requires at least as many detectors as targeted modes [84], although, for long-lived signals, the detector motion can also help in breaking degeneracies by changing the detector's pattern function over time [85]. Theory-independent null-stream methods benefit from combining multiple detectors as well [95, 97]. Overall, this test presents a strong synergy between detectors, where combining detectors in a network, and in particular combining ET with one or two CE observatories, would directly improve our ability to disentangle additional polarizations [85].

Take home message

- Synergetic observation of stellar and intermediate BBH systems by ET and LISA can bound GR by an order of magnitude better than either observatories.
- Joint observation by ET and CE is a unique opportunity to measure polarization modes of the waves and constrain alternative gravity theories.
- Dipolar-radiation test is boosted by combining ET with milli-Hertz and Deci-Hertz GW observatories.

JCAP03(2026)081

6.5 Hubble tension and cosmography

Cosmography and Cosmology: Synergies with CE and LISA

- What are the key improvements that a 3G network of Earth-based GW observatories can bring to cosmology?
- Can the synergy among GW experiments be also crucial for other observatories, particularly in the context of multi-messenger astronomy?

The determination of the expansion history of the Universe largely benefits from the combination of different datasets, as in the current "concordance" scenario. The use of GW sirens provides a new player in this landscape, which will be further bolstered by the synergy among future GW observatories.

The discrepancy between local [1788, 2504–2507] and CMB-based [591] measurements of the Hubble constant H_0 either points to unresolved systematics or new physics. As such, the field of cosmology greatly benefits from new classes of cosmological sources for which it is possible to measure the Universe's expansion. The presence of a network of next-generation GW observatories will give us access to a plethora of sources at cosmological scales, thus allowing us to corroborate the origin of the H_0 tension. In the case of new physics, the possibility of determining H_0 to sub-percent level with tracers complementary to EM and CMB observations would be of paramount importance.

Furthermore, the increased detection horizon of 3G observatories, as shown in figure 105, will give us access to thousands of GW events from the dark matter-dominated era (beyond redshift 0.3). Contrary to current generation GW observatories at their designed sensitivity, 3G generation observatories will allow us to constrain cosmological parameters beyond H_0 such as the dark matter fraction Ω_m. GWs can further allow us to probe the presence of dark energy, through the imprint of its EOS on rate of expansion of the Universe, and more importantly the phenomenon of "modified GW propagation" taking place whenever GR is modified at cosmological scales, as discussed in section 3.3.2. The coordination of ET with a network of next-generation GW observatories will significantly boost current techniques for GW cosmology and also allow for studies of GW sources as large-scale structure tracers that are currently impossible. In general, we can identify several common benefits for GW cosmology: *(i)* the improved distance reach allowing to target high-redshift sources; *(ii)* the improved localization capabilities of a network of GW observatories; *(iii)* the overall boost in the number of detections per observation time and *(iv)* the possibility of multi-band observations and constraints. We discuss how these common benefits will impact future prospects for GW cosmology.

6.5.1 Bright sirens cosmology

Localization is of crucial importance for GW cosmology. A precise localization of GW events can allow us to promptly identify a possible EM counterpart but also statistically identify the source galaxy from galaxy surveys.

JCAP03(2026)081

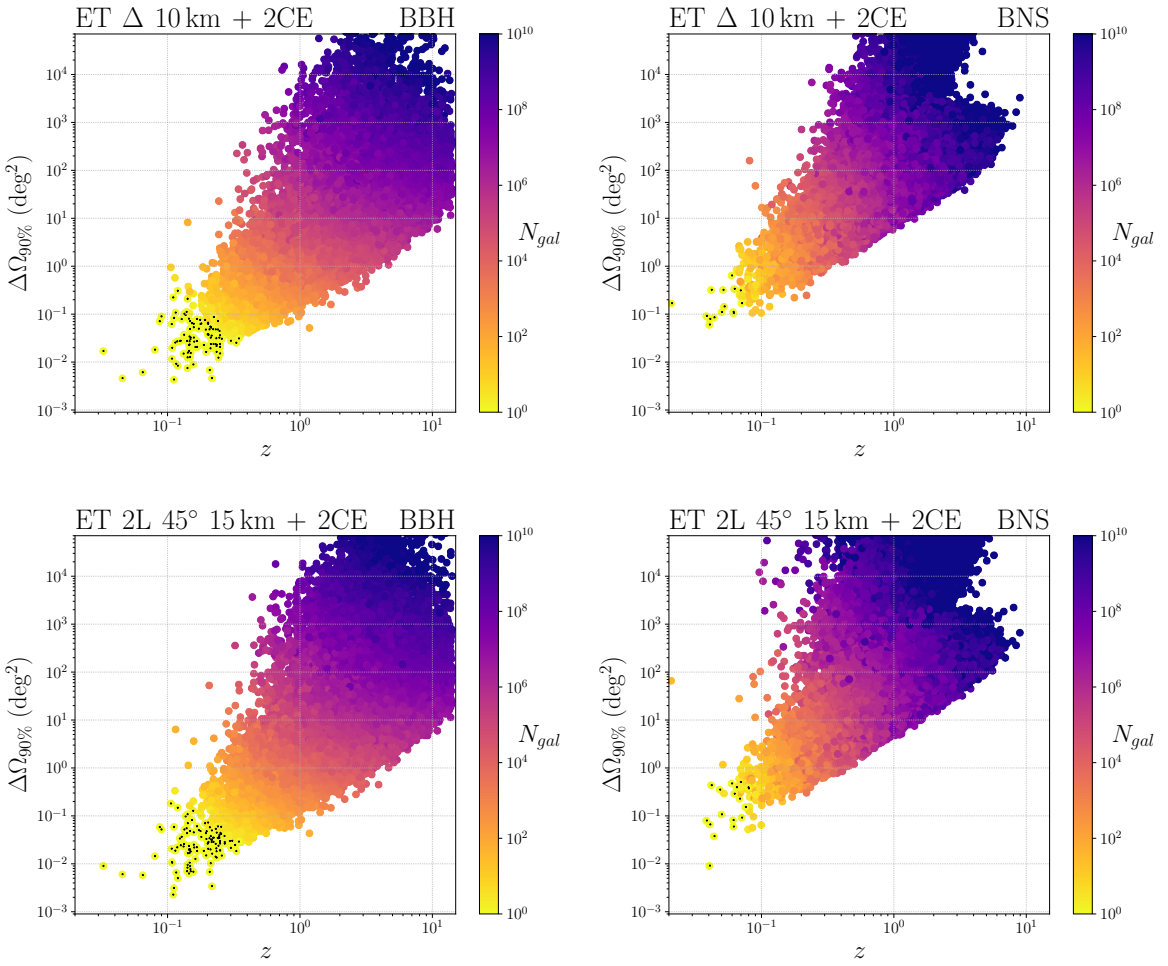

Figure 113. Localization capabilities for BBH (left panels) and BNS (right panels) of ET in its triangular and 2L configurations (first and second rows respectively), in a network with two CE. The color scale denotes the number of galaxies expected in the 90% localization volume. Events marked with black dots are localized to one galaxy only.

Figure 113 shows the localization capabilities of ET in synergy with two CE observatories, for BBH and BNS respectively.[56] In particular, we show the 90% sky localization area as a function of redshift, while the color refers to the number of galaxies contained in the localization volume, assuming a constant galaxy density of 10^{-2} galaxies/Mpc^3, where the galaxy density is derived integrating the Schechter function of ref. [2508] from 10^9 to 10^{12} solar masses. Events with a single host galaxy in their localization volume are further marked with a black dot. Specifically, ET triangle (2L) operating with 2CE is able to localize within a volume containing a single galaxy (for galaxy in the above mass range), 47 (55) BBH mergers per year at redshifts below 0.4 and 17 (16) BNS mergers per year at redshifts below 0.1.[57]

[56] We refer to ref. [16] for the details on the catalogs and software used.

[57] We underline again that these numbers are subject to uncertainties dominated by the limited knowledge of the local merger rate of compact objects. For BNS mergers, taking into account the absence, to date, of detection in the current O4 run, we can consider these numbers as an upper limit, see also footnote 21 on page 94.

JCAP03(2026)081

In particular, BNS systems are targets for follow-up multimessenger campaigns, where sky localization plays a major role. The synergy with CE brings a dramatic improvement in localization: ref. [16] finds that the number of sources localized to better than 10 deg^2 increases from 8 to ~ 6500 for ET in the triangular configuration, and from 25 to ~ 9800 for ET in the 2L configuration; for localizations better than 100 deg^2 the number of sources increases from 184 to $\sim 10^5$ for ET in the triangular configuration, and from 559 to $\sim 1.5 \times 10^5$ for ET in the 2L configuration. As shown in figure 113 there is subset of $\mathcal{O}(10)$ well-localized GW events for which it will be possible to identify the host galaxy solely from the GW localization volume, without the need of any transient EM counterpart. This is not currently possible with current-generation GW detectors.

For the impact on the measurement of H_0, it would already be possible to obtain sub-percent accuracy with one year of observations of ET alone (see section 6.4 of [16]), if a precise redshift measurement following the localization of the source through the kilonova emission produced by BNS mergers in the optical band can be obtained. In particular, this can be possible in synergy with the Vera Rubin Observatory [16] for sources up to redshift $z \sim 0.3 - 0.4$. The addition of two CE detectors would boost this accuracy to an unprecedented level, as well as decreasing the time required to reach such a goal (even to just a few days of observations). Even more interestingly, we note that besides H_0, other parameters affecting the distance-redshift relation might not be constrained to better than a few percent with ET alone. In particular, ref. [16] finds that the matter density $\Omega_{\rm M}$ would be constrained at $20 - 30\%$, the dark energy EOS parameter w_0 at $\geq 10\%$ and the parameter Ξ_0 describing modified GW propagation [1257, 1259] at $\sim 3\%$. Crucially, the addition of CE would allow to reach percent or sub-percent level accuracy for all these parameters, allowing to reconstruct the local expansion history in full generality (as well as to provide a stringent test of ΛCDM) rather than just the local value of the Hubble constant [1172].

6.5.2 Dark sirens cosmology

3G interferometers are expected to detect most of the stellar BBHs merging up to $z \sim 100$ [16, 1167]. Albeit no associated EM counterpart is emitted, the abundance of such dark sirens allows for statistical methods, discussed in section 3.3.1.2, to become efficient. Within this framework, the localisation power plays a crucial role in the precision that this approach can reach, as galaxy catalogues are employed to counterbalance the lack of the source's redshift [1143–1145, 1147, 1160, 1161, 1185, 1206, 2509–2511]. While ET alone might not be able to pin down the sky position of a large number GW source accurately enough, a network of ET and CE can restrict the potential hosts to a few candidates for a large number of events. A sub-percent H_0 measurement can confidently be attained by employing only the loudest dark sirens observed in 1 yr of observations [1185]. Furthermore, we expect to localise a few tens of GW events per year accurately enough that only one host galaxy falls inside the credible region (left panels of figure 113). These unique events, which contain most of the information, would constrain H_0 down to $\mathcal{O}(1\%)$ precision alone [1185, 2511] if provided with complete galaxy catalogues.

Dark sirens detected by 3G detectors will play a crucial role in cosmology even in the absence of any galaxy survey information. As discussed in section 3.3.1.2, by exploiting the

JCAP03(2026)081

relation $m_{\rm det} = (1+z)m$ between detector-frame mass $m_{\rm det}$ and the actual ("source-frame") mass m, it is possible to obtain a statistical redshift estimation of the source [1151, 1152] and jointly fit for the source mass spectrum and cosmological expansion parameters [1147, 1153, 1156, 1158, 1160, 1161]. Dark sirens that are employed for this type of analysis have been recently named "spectral sirens" [1156]. To reach a percent-level estimate of H_0, we would require at least thousands of spectral sirens [1147, 1153, 1158] that could be provided at the end of the planned observing runs in 2027 for current GW detectors. While current GW detectors could already provide in the next years a percent-level measure of H_0 with spectral sirens, they will not provide a high enough number of sources to consistently check for systematics in the H_0 measure that could arise from poor calibration of mass distribution models [1200]. In contrast, 3G observatories will make accurate and precise cosmology with spectral sirens possible; 3G observatories will provide $\mathcal{O}(10^5)$ GW sources at all the cosmic times in just one year of observation, as we see also from figure 105. The large number of GW detections will allow us to perform spectral siren analyses with independent subsets of thousands of GW sources. The use of an independent subset of GW observations, divided accordingly to their mass and distance from us, will provide an in-depth understanding on the most critical assumptions that could possibly introduce systematics in the estimate of H_0.

Another possibility is the use of GWs as tracers of the Large Scale Structures, and the extraction of cosmological information from their two-point cross-correlation with galaxy surveys [1318, 1319, 1323, 1324, 1337, 1338, 1361, 2512–2515], see the discussion in section 3.4.1. The main limitation of this method comes from the poor angular resolution of GW sources as compared to galaxies. In particular, the minimum resolution of the GW survey determines a limiting scale in the angular power spectrum [1318, 1319, 1323, 1324], $\ell_{\rm max} \sim 180^\circ/\Delta\Omega_{\rm max}^{1/2}$ with $\Delta\Omega_{\rm max}$ being the maximum resolution of the instrument. While the angular resolution of ET alone corresponds to roughly $\Delta\Omega_{\rm max} \sim 0.1\,{\rm deg}^2$, hence a maximum multipole of at most ~ 300 only in a local redshift shell (up to $z \sim 0.2$), from figure 113 we see that the addition of CE could allow to reach $\Delta\Omega_{\rm max} \lesssim 0.01\,{\rm deg}^2$, corresponding to a maximum multipole of ≥ 1800 at low redshift, and a maximum multipole of ≥ 300 up to redshift $z \sim 1$. In practice, going to high multipoles would require to model non-linear scales; however, refs. [1319, 1338] find that sub-percent accuracy on H_0 could already be achieved with a cut $\ell_{\rm max} = 300$ which is reachable with ET in combination with CE.

Finally another dark sirens method which can be applied to 3G observatories, consists in the simultaneous estimation of cosmological parameters and the EOS of NSs, as discussed in section 3.3.1.2. A network of 3G observatories will have the potential to determine the EOS of NSs with great accuracy, in turns providing an associated redshift measurements for all compact binary mergers including a NS. Such a method does not require an EM counterpart and could deliver constraints on H_0 comparable to other siren methodologies [1140, 1230, 1233, 2516].

6.5.3 Multi-band sources

The presence of multiple GW observatories covering complementary frequency ranges will open further unique possibilities. ET detection horizon is complementary, in terms of source masses, to LISA, as well as to the Deci-Hz detectors discussed in section 6.1. This

JCAP03(2026)081

complementarity is crucial for GW cosmology for two reasons. These low-frequency detectors could provide early-warning alerts to prepare ET for the detection of the merger of BNSs and SOBBHs [2510]. They will scan the Universe for a population of BBHs with masses $\gtrsim 10^3 M_\odot$, on which we currently lack knowledge. If this population of GW sources exists, we will be able to perform GW cosmology with an independent set of data that can be used to corroborate possible systematics present in ET [2517].

In addition, there are classes of compact objects for which detections of the same source in different experiments will be possible. In particular, BBHs originating from massive stars, which exceed the pair-instability mass gap and with masses in the range $120M_\odot - 300M_\odot$, are considered prime dark siren candidates for GW observations across multiple frequency bands [2510, 2518, 2519]. The prolonged inspiral signals emitted by these systems can be observed by LISA, or even better by Deci-Hz detectors, while the later stages of inspiral and merger will be detected by ET. The combination of the observations from LISA and ET will improve the sky localization of these sources by a factor $\mathcal{O}(10-100)$ compared to those obtained with the same sources using only ET. Ref. [2510] finds that with 4 years of LISA observation this multiband approach may allow for a $\mathcal{O}(2\%)$ estimate of the Hubble constant H_0 with $\mathcal{O}(10)$ detected sources. An even better precision is expected from Deci-Hz detectors, which can follow the inspiral up to minutes before merger [2520, 2521].

Take home message

The synergy among different Earth-based GW observatories can be a game-changer for late-time cosmology with resolved sources, due to the improved localization capabilities which are crucial for both bright and dark siren cosmology. The interplay with GW observatories in other frequency bands will further allow to enlarge the spectrum of GW sources used for cosmology and to target well-localized multi-band sources.

6.6 The origin of supermassive black holes

The Link Between Stellar and Supermassive Black Holes

- What can joint observations by ET and LISA reveal about the nature of the seed black holes that eventually grow supermassive? Are stellar-mass black holes, formed at cosmic dawn, the sole building blocks of the supermassive black holes powering quasars observed as early as redshift $z \sim 11$, and now residing almost ubiquitously in the centers of quiescent galaxies?
- What can ET and LISA tell us about intermediate-mass black holes in the range $10^2 - 10^5\, M_\odot$, which bridges the gap between the stellar and the supermassive black holes?

The discovery of rare quasars at redshifts as high as $z \sim 11$ [2126, 2522–2529], of the large population of active galactic nuclei (AGN) emerging at $z \lesssim 6$ and extending to

JCAP03(2026)081

$z \sim 1$ [2530], and of dark massive objects in the nuclei of today's quiescent galaxies [2531] provides evidence of the ubiquity of supermassive black holes (SMBHs) in the near and far Universe. Understanding the origin of SMBHs is important and goes hand in hand with understanding the formation and evolution of stars and galaxies, which is a process rooted in our current model of cosmic structure formation [2532].

The most massive BH binary currently detected by GW observations, GW231123, resulted in a final BH with a mass of about $225\,M_\odot$ [2533], providing evidence of hierarchical assembly of heavy BHs from stellar-mass parents. ET on Earth and LISA from space will probe an immense volume of the Universe as both observatories have sensitivities to detect GW signals from merging binaries out to $z \sim 15 - 20$. This capability enables the measurement of black hole masses across the largely unexplored segment of the spectrum, ranging from about $10\,M_\odot$ up to $10^7\,M_\odot$, and over cosmic time, offering crucial insights into when, where and how SMBHs form from their seeds (see [2532, 2534, 2535], for detailed reviews). ET will have the capability of discovering the earliest black holes, relics of the first population III stars. Inside gas-rich regions of the host halos, some of these black holes can rapidly grow via accretion and mergers becoming viable seeds for SMBHs [2536–2539]. This establishes a close connection between stellar-mass and supermassive black holes. While ET can reveal the existence of the first seeds, LISA will trace their subsequent growth, uncovering the evolving population of accreting light seeds over cosmic time [2540].

Independent, synergetic observations of the two different populations, the stellar and massive ones, will help breaking degeneracies among different evolution pathways. This is achieved by matching, in a multi-dimensional space and within a defined theoretical framework, the information resulting from the measurements of the black hole masses, spins (when possible) and redshift of individual sources, and by confronting the relative rates of coalescence events detected by ET and LISA, respectively.

6.6.1 Seed black holes

In section 4.7 we presented a detailed overview of the latest advances in understanding the properties of the first stars, known as population III stars, forming in the earliest collapsing dark matter halos of $10^{5-6}\,M_\odot$ at $z \lesssim 30$. Their initial mass spectrum is unknown and theoretical investigations indicate that it is in the range from 1 $M_\odot$ to several $10^2\,M_\odot$. This population is expected to dominate at $z > 13$ and to persist down to $z \sim 6$, albeit in subdominant fractions compared to the growing population II stars. Despite the increasing number of hints, recently provided by the JWST telescope, on possible indications of population III star's signatures in the spectra of high redshift galaxies or in lensed sources [2003, 2004, 2541, 2542], direct EM observations of single stars are beyond foreseen capabilities.

The properties of population III stars are encoded in those of their relics, i.e. the black holes that ET can uncover, see section 4.7. The role of ET is therefore central in inferring the properties of these first stars, but not only. These early black holes are expected to represent the channel of formation of the light seeds of up to a few to several $10^2 M_\odot$ [2532]. These may not be the only seeds to grow SMBHs. Heavy seeds of $10^{3-5}\,M_\odot$ have been also hypothesized, resulting either form direct collapse of massive gas clouds, via runaway stellar mergers or hierarchical black hole mergers [1551, 2537]. LISA can observe these heavy

JCAP03(2026)081

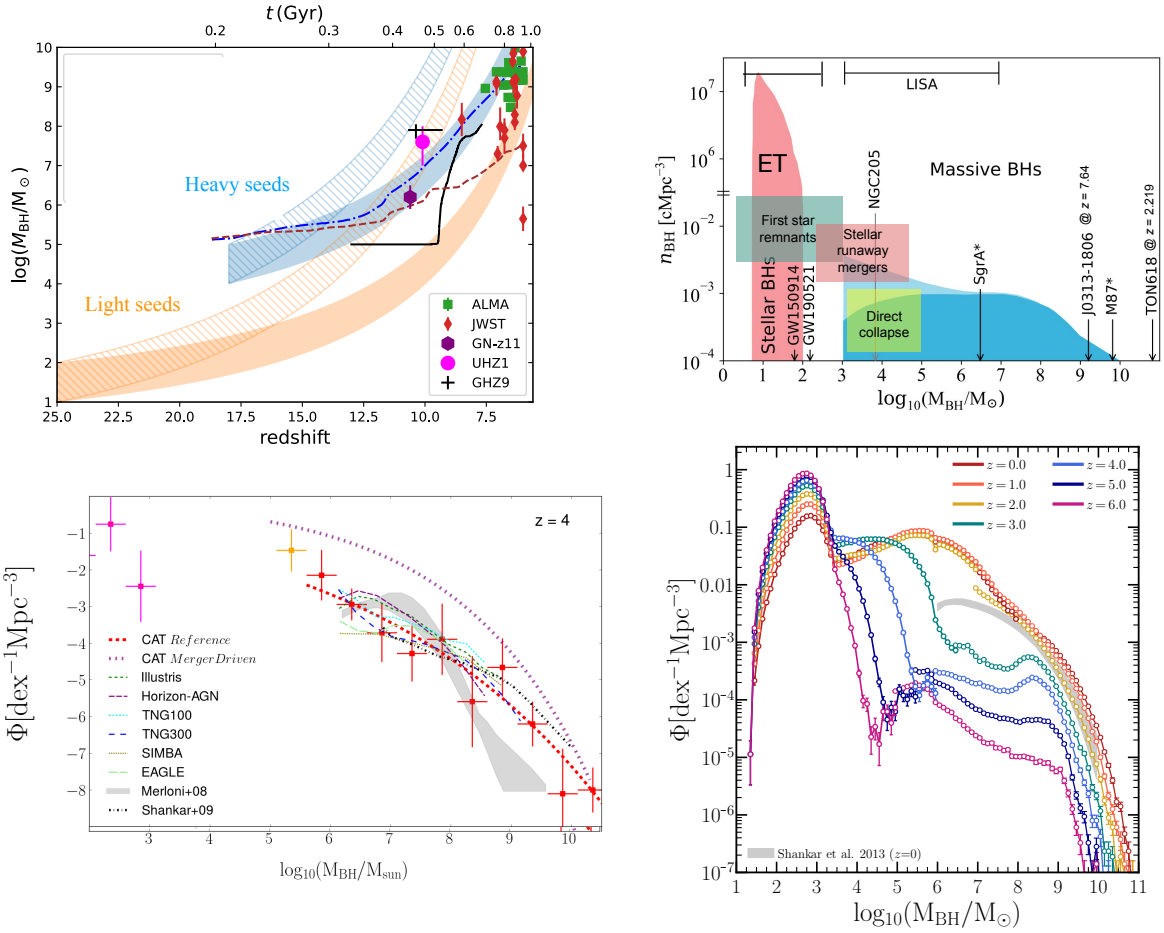

Figure 114. *Upper left panel:* tracks of BH growth, for different initial *seed* masses assuming uninterrupted accretion at the Eddington rate and at rates twice above this limit. The different colored symbols labeled in the figure refer to $z > 6$ observations of quasars by ALMA (green squares [2543]) and JWST (red diamonds [2524, 2528, 2544–2546]), including the $z \sim 10$ massive black holes in UHZ1 (magenta circle [2126]), GHZ9 (black cross [2527]) and the candidate super-Eddington accreting black hole in GN−z11 (violet hexagon [2127]). Light seeds can explain these quasars if they accrete at a super-Eddington rate. Heavy seeds, forming at lower redshifts, do not necessarily need sustained super-Eddington accretion. There is a debate whether sustained accretion above the Eddington limit is likely in high-redshift galaxies [2529, 2539, 2547–2550]. The black, blue and red tracks refer to state-of-the-art high-resolution cosmological zoom-in simulations [2550, 2551] where a $10^5 M_\odot$ black hole was implanted at $z = 10$ and let evolve including accretion and feedback. *Upper right panel:* cartoon sketching the mass spectrum of black holes and the different formation paths. Arrows and labels indicate selected quasars, the Milky Way black hole, Sgr A*, [2552, 2553] M87 [2554], and the post-merger mass of GW150914 and GW190521, the first and the most massive coalescence events detected to date by LVK, respectively [1509, 2555]. Shown are the windows of exploration of ET and LISA (adapted from [2532]. Reproduced from [2532], with permission from Springer Nature.). *Lower left panel:* BH mass spectrum at $z = 4$ from [2539] as inferred from a suite of semi-analytical models and numerical simulations to show the still large theoretical uncertainties in predicting BH evolution. Data points show the distribution of light (magenta) and heavy (red, orange) BH seeds, with the best fit for the distribution of heavy seeds in red and violet dotted lines, and the results from large-scale cosmological simulations: Illustris (dark green, cyan, and blue [2556, 2557]), SIMBA (olive [2558]), and EAGLE (light green [2559]). The observational constraints by [2560] and [2561] are shown in the grey shaded area and black dashed-dotted lines. Reproduced with permission from [2539]. *Lower right panel:* evolution of the BH mass function from the semi-analytical model L-Galaxies [2562]. The figure shows how the intermediate-mass range is being progressively filled due to the growth of light seeds from population III relics (Courtesy of Izquierdo Villalba).

JCAP03(2026)081

seeds, whose relative contribution in explaining the formation of high-z quasars ($z > 4$) is under debate [2534, 2535, 2563].

The upper left panel of figure 114 illustrates the concept of black hole growth from light seeds and heavy seeds in selected mass ranges. In the same figure (upper right panel) we show the extension of the BH mass spectrum, known as of today, indicating the main formation pathways. Note the presence of a desert around $10^{2-3}\,M_\odot$, and the uncertainty in the rise or decline of mass distribution around $10^{3-5} M_\odot$, where intermediate mass black holes (IMBHs) sit [2090, 2091]. IMBHs are in the midst of the high-end tail of the stellar BH mass distribution and the low-end tail of the SMBH mass distribution. At present, whether a discontinuity exists in the families of stellar and supermassive BHs, related to the existence of uncorrelated physical processes, is not known. In this regard, the lower right panel of figure 114 shows the evolution of the BH mass distribution as a function of redshift from the semi-analytical cosmological model L-Galaxies [2562] that describes the formation and evolution of SMBHs from light and heavy seeds. This model indicates that the IMBH segment is being progressively filled by growing light seeds which evolve to account for the vast population of AGN, with heavy seeds partially explaining the rare high-z quasars.

There are large theoretical uncertainties related to the way the seeding process and seed growth is treated in inferring the BH mass spectrum as a function of redshift. This is illustrated in the left lower panel of figure 114, taken from [2539]. Different models give different predictions on the shape and normalization of the mass function [2539, 2564–2568]. Therefore, future GW observations will be key to help reducing these uncertainties, jointly with forthcoming deeper studies and observations of quasars and AGN in the EM sector.

6.6.2 Synergies between ET and LISA

Participating in the formation, growth, and assembly of cosmic structures, massive black hole in merging galaxies form binaries that coalesce, becoming sources of low-frequency GWs [330, 512]. LISA, operating from below 0.1 mHz to about 1 Hz, aims at detecting the signals from these sources in the segment of the mass spectrum between about $10^4\,M_\odot$ and $10^7\,M_\odot$, out to redshift $z \sim 10 - 15$. The LISA's cosmic horizon together with ET's horizon are shown in figure 115.

Signals. The GW signals detectable by LISA encode key information on the black hole source-frame masses, luminosity distance, and when sufficiently loud the spins [330]. GW signals from binaries of $\sim 10^4 - 10^5\,M_\odot$ feature an inspiral phase lasting several months before merger, with median signal-to-noise ratios (SNRs) typically reaching up to $\lesssim 100$. The source-frame masses in this case can be determined with uncertainties from 10% to 100%. ET will measure with comparable accuracies the physical parameters of potential light seeds, whose signal display only few inspiral-cycles before final plunge [1181]. Below $z \sim 8$, the inspiral, merger and ringdown signal of LISA's binaries contains all information to enable accurate measurements of the source-frame masses at the level of 10% and effective spin with accuracy of 1%. At $z \sim 2$, SNRs are as large as a few thousands, with black hole masses and luminosity distances measured with accuracy at the level of 0.1%, and the spin

JCAP03(2026)081

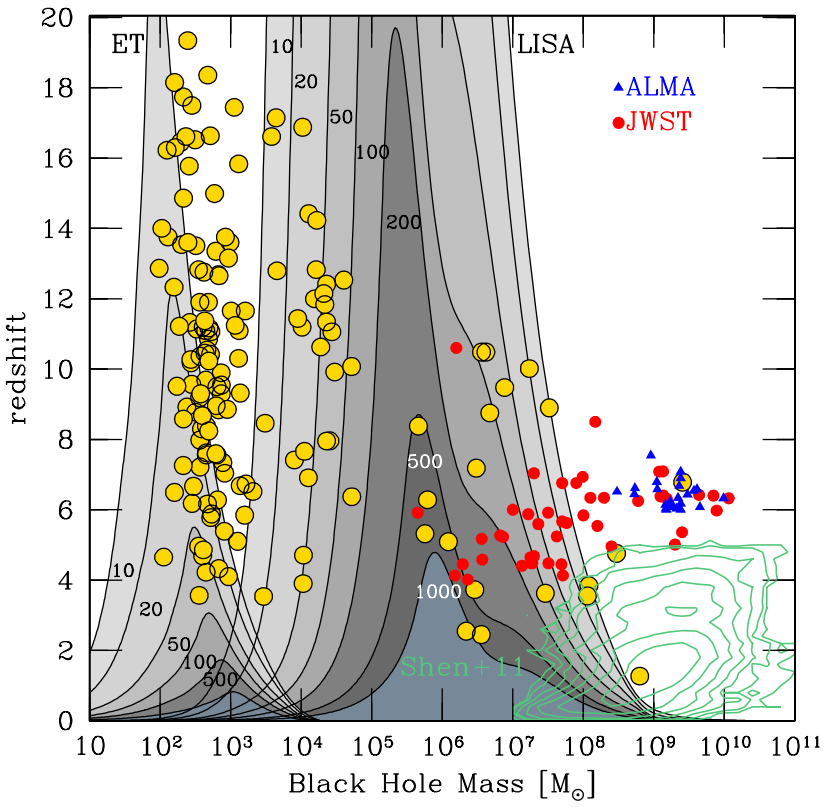

Figure 115. The ET and LISA cosmic horizons. The figure shows contour lines of constant signal-to-noise ratio (SNR) in the plane redshift versus total mass of the black hole binaries, as measured in the source frame. Binaries have all mass ratio 0.5. Yellow dots denote loci of BH mergers extracted from the semi-analytical model of [2540], which tracks the evolution of light and heavy seeds forming in merging halos. Light seeds form at $z \sim 20 - 30$ as relics of population III stars in molecular cooling dark matter halos of $10^6\,M_\odot$. Heavy seeds form later ($z \sim 10 - 20$) in atomic cooling halos of $10^8\,M_\odot$ under contrived conditions (see the review by [2535] and references therein). The bulk of the merging black holes in LISA come from the growing light seed population that ET can detect when seeds form in binaries. Red dots and blue triangles denote the quasars observed at $4 < z < 11$, from JWST [2524, 2528, 2544–2546] and ALMA [2543], respectively. Green contour lines depicting the vast population of AGN are from [2530].

of the primary black hole, which provides clues on the way accretion proceeded [512, 1550], with an absolute error of 1 part in 10^3 [330].[58]

Rates. The ET merger rate density associated to population III stars (and in turn to potential seeds) has been estimated to range from 0.1 to about $200\,\mathrm{yr}^{-1}\,\mathrm{Gpc}^{-3}$, extending from $z \sim 15$ to 6, corresponding to a detection rate of about ten to hundreds of events per year in ET

[58] It should be observed that many LISA massive black hole mergers are expected to occur in gas-rich ("dirty") environments. Gas-induced effects, such as those from accretion disks, generally introduce waveform dephasing measurable during the end of the inspiral, the merger, and post-merger phases. This is known to be critical for extreme mass ratio inspirals (EMRIs), which however are sources unique to LISA. For the high-redshift massive black holes observed by LISA during their long inspiral, and which could then later merge in the ET band, these environmental effects are smaller than the statistical uncertainties. For detailed discussions on environmental effects in GW astrophysics, see [2569].

JCAP03(2026)081

(e.g. [1673, 1674, 2049, 2056, 2063, 2071, 2073, 2570]). The LISA merger rates range between a few to several tens per year, with the uncertainties in these values rooted in the largely unknown process of pairing of massive black holes down to the milli-parsec scale below which GWs drive the late inspiral and final plunge [2540, 2562, 2565, 2571–2575]. The physics of binary formation in LISA is completely different from that of ET stellar binaries, as it occurs via galaxy mergers: orbit's sinking in a galactic collision is controlled by the complex interaction black holes have with their surrounding dark matter, stars and gas, during a major or/and minor galaxy merger [512]. LISA rates at $z \gtrsim 8$ depends largely on how short is the sinking time compared to the "then" Hubble time, and depending on the model rates range again from a few to several per year [2562, 2574, 2575].

ET and LISA together. In figure 115 we show the synergy between ET and LISA. In [2540], a semi-analytical cosmological model was developed, aimed at reproducing typical quasars observed at redshift 8 and 2. The seeding mechanisms include both light and heavy seeds and merging binaries (yellow dots in the figure) form during halo-halo mergers, under the hypothesis that dynamical interactions lead to their formation and pairing. The model shows that most of the LISA events are rooted in the process of formation of stellar black holes from population III stars, with only a few resulting from heavy seeds.

Comparing GW merger events of $\sim 10^2\, M_\odot$ binaries at $z \sim 10 - 14$ detected by ET, with events of $\sim 10^4 - 10^5\, M_\odot$ at comparable or lower redshifts with LISA (just on the edge of the left side of the LISA waterfall plot shown in figure 115) paves the way for identifying light seeds as progenitors of SMBHs. Lack of ET high-z events around a few $10^2 M_\odot$ could indicate that either they rarely form, or that they rarely pair in binaries which merge shortly after. From the LISA perspective this might indicate that heavy seeds only are the progenitor of the SMBHs or that light seeds grow at a very fast (super-Eddington) rate, following their formation without experiencing mergers. All of this needs to be quantified through careful modeling of black hole cosmic formation and evolution.

6.6.3 IMBH populations across frequency bandwidths and detectors

Intermediate mass black holes (IMBHs) in the mass range between a few hundreds $M_\odot$ and $\mathcal{O}(10^5)\, M_\odot$, bridging the known stellar and supermassive BHs, are ideal sources to exploit the advantages of having more than one detector in different frequency bands. As described in section 4.8, IMBHs are expected to form as outcome of close and repeated dynamical encounters among stars or stellar black holes inside dense and massive clusters [1491, 2129, 2131]. IMBHs can also from in the collapse of gaseous clouds in protogalaxies [2576], or from gaseous accretion onto massive stellar remnants originating from the first stars [2577]. Despite the plethora of formation scenarios and the growing evidence of IMBH candidates in dwarf galaxies [2090, 2091], the existence of IMBHs and their role in galaxies, whether ubiquitous or rare, is still unclear and actively debated. In these regards, the detection of GWs from merging IMBHs is key to understanding where, when, and how IMBHs form along cosmic history.

ET can detect equal-mass IMBH binaries with source-frame masses of $\lesssim 10^3\, \mathrm{M}_\odot$ at redshift $z \lesssim 7$ [16], and IMBH-BH systems having a stellar BH and a primary of $\sim 10^3\, M_\odot$, at redshift $z \gtrsim 1$ [1538]. Detecting IMBH and IMBH-BH binaries (the last referred also as

JCAP03(2026)081

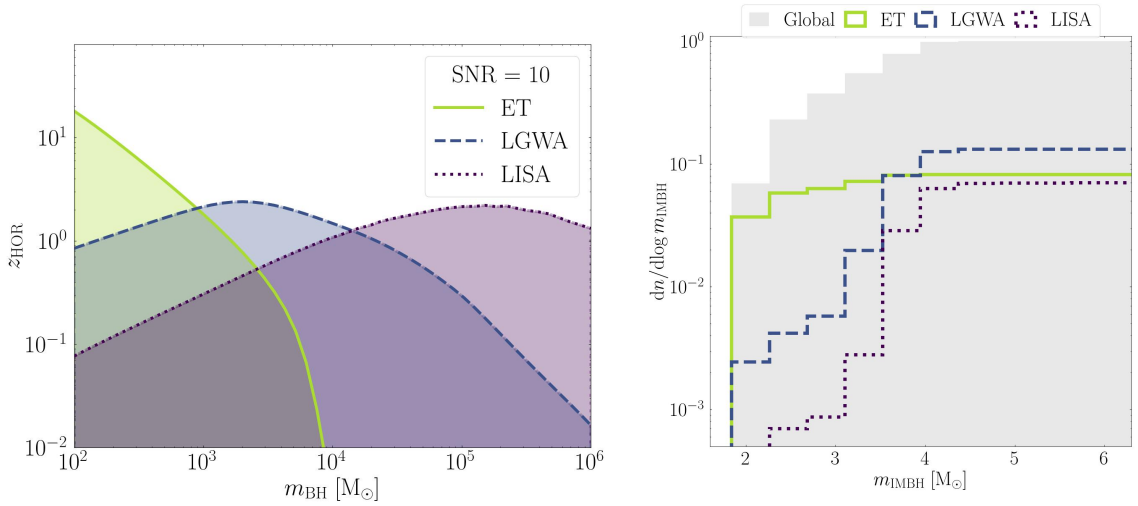

Figure 116. *Left panel:* horizon redshift for IMRIs involving a stellar BH of $30M_\odot$ as a function of the mass of the more massive primary $m_{\rm IMBH}$. Detection is set at SNR=15 using the GWFish tool [291] for ET (green straight curve), LGWA (blue dashed curve), and LISA (purple dotted curve). *Right panel:* cumulative mass distribution of IMRI detection versus the IMBH mass. These systems are dynamically formed in young, globular, and nuclear clusters and their overall population is shown by the filled grey histogram. The detectable sub-population of IMRIs are shown for ET, LGWA and LISA (as in the legend). Models are obtained from combined population synthesis simulations performed with the BPop code [1528] and parameter estimation performed with GWFish. Adapted from Arca Sedda (in prep).

intermediate-mass ratio inspirals or IMRIs) will provide us information about the efficiency of dynamical processes in population I, II, and III star clusters in producing IMBHs.

As discussed above (see also figure 115), the horizon reach of ET for IMBHs of mass close to $(1-5)\times10^2\,M_\odot$ extends up to $z\sim10$ [16, 1181, 1569]. However, binary IMBHs can also be present at lower redshifts. With ET operating with two CEs in network, we can measure the mass of an equal-mass IMBH binary of $\sim10^3M_\odot$ with accuracy of $\lesssim0.1\%$ (1%) at redshift $z=0.5$ (2) [1569]. Such a network can localise binaries at $z=0.1-0.5$ with mass ratio $q\sim0.1$ and primary mass of $\sim(5\times10^2-10^3)\,M_\odot$ within an angular localization $\Delta\Omega\sim(0.01-1)\,{\rm deg}^2$ [1569]. Good localisation and accurate measurements of the properties of merging components can help distinguishing both the environment nurturing the IMBH growth and the IMBH formation channel.

At $z\lesssim1$, ET can detect signals from binaries made of an IMBH and a stellar BH, which could in principle also be detected by low-frequency observatories such as LISA or Deci-Hz detectors. This is illustrated in figure 104. IMRI binaries are exquisite probes of the physics of formation of IMBH in dense environments as these systems form exclusively from the dynamical channel. Combining different detectors operating independently at different frequencies makes it possible to cover the IMBH mass range fully and to place stringent constraints on the IMBH mass distribution, shedding light on the origin of IMBHs. As an example, the right panel of figure 116 shows the mass distribution of a population of IMRIs resulting from dynamical interaction in dense young, globular, and nuclear clusters modeled

JCAP03(2026)081

with the B-POP population synthesis model [1528] and the corresponding distribution of detectable mergers in ET and other detectors, while the left panel of the figure shows the horizon redshift for ET, LISA, and LGWA in the case of an IMRI hosting a stellar BH of $30\,M_\odot$ inspiralling/merging with a primary in the mass-range $(10^2 - 10^6)\,M_\odot$. As shown in figure 116, an IMRI can be detected during the inspral phase in LISA and at merger in LGWA. The cumulative mass distribution for this selected IMRI (right panel of figure 116) shows the saturation mass in the three detectors. Finally, it is interesting to remark that with LGWA and Deci-Hz detectors we have the possibility to probe the region of the IMBH mass spectrum that is poorly covered by ET or LISA, i.e. roughly $(5 \times 10^3 - 10^4)\,M_\odot$ [1470, 2412, 2578].

Joint multi-band observations of the same event will be possible for $(10^2 - 10^4)M_\odot$ binaries out to redshift $z \sim 2 - 4$, enhancing the ability to carry on precise measurements of the source parameters at such high redshifts [2579]. Multi-band detection of distant lower (higher) mass binaries would be instead limited by the sensitivity for LISA at frequencies around and above 0.1 Hz (for ET/CE at frequencies around and below 3 Hz).

TAKE HOME MESSAGE

- ET WILL BE UNIQUELY CAPABLE OF DETECTING BLACK HOLE RELICS FROM THE FIRST GENERATION OF MASSIVE STARS. ITS SENSITIVITY WILL ALLOW GOOD MEASUREMENTS OF THEIR MASSES AND REDSHIFTS, OFFERING VALUABLE INSIGHTS INTO THE FORMATION OF PRISTINE STARS IN BINARY SYSTEMS. SOME OF THESE EARLY BLACK HOLES MAY SERVE AS "LIGHT" SEEDS IN THE HIERARCHICAL GROWTH OF MASSIVE AND SUPERMASSIVE BLACK HOLES.
- BY COMPARING MERGER EVENTS OBSERVED BY ET AND LISA, EACH SENSITIVE TO DIFFERENT MASS INTERVALS — AROUND $100\,M_\odot$ FOR ET AND $10^5 M_\odot$ FOR LISA –IT WILL BE POSSIBLE TO STATISTICALLY PROBE THE MECHANISMS OF BLACK HOLE SEEDING AND GROWTH.
- INTERMEDIATE-MASS BLACK HOLES OF $10^3 - 10^4\,M_\odot$ PAIRED WITH STELLAR BLACK HOLE COMPANIONS, ARE UNIQUE PROBES OF THE DYNAMICAL FORMATION CHANNEL. ET, IN SYNERGY WITH LOWER-FREQUENCY DETECTORS, OFFERS A DISTINCTIVE OPPORTUNITY TO DETECT THESE STILL ELUSIVE BLACK HOLES.

JCAP03(2026)081

6.7 Early Universe cosmology

Cosmological Backgrounds

- What particle physics models predict early Universe phase transitions or the formation of cosmic strings? Can we precisely pin down the properties of such models by measuring the GWs they produce, using ET in synergy with other GW observatories?
- What is the source of cosmic inflation? Can it generate a broad spectrum of SGWB with a sufficiently large amplitude to be detected by ET, and by other GW experiments operating at lower frequencies?
- Can we extract information on the early Universe cosmic history (before Big Bang nucleosynthesis) by precisely measuring the frequency dependence of the stochastic GW background produced by primordial sources? Does a synergy between ET and other instruments offer any advantage in answering this question?
- What is the source of the GW background for which evidence was recently found by several PTA collaborations? If it has a primordial origin in terms of cosmic phase transitions, inflation, or cosmic strings, can a future detection by ET help in characterizing its origin?

Stochastic GW backgrounds can be detected across various frequency bands and have an astrophysical or cosmological origin [60, 537–540]. In particular, as discussed in detail in section 3.2, the early Universe immediately after the Big Bang could create a stochastic GW background (SGWB), through mechanisms such as the amplification of vacuum fluctuations in models beyond the single-field slow-roll paradigm, first-order phase transitions, cosmic strings, or domain walls. From the observed spectrum of the backgrounds, ET could learn about the physical processes that generated them and hence obtain a picture of the Universe at the earliest moments of its creation. The sensitivity to stochastic backgrounds of ET as a single observatory, both in the triangle and in the 2L configurations, are discussed in detail in section 10.5, see in particular figure 195, and in section 11.6 where, for the triangle configuration, is also discussed the use of the null stream, see section 11.6.1, as well as the potential caveat of the masking effect of correlated noise, see section 11.6.2. The correlation of ET with other ground-based observatories would help rule out whether the observed backgrounds originate from instrumental or environmental disturbances. For example, ET in conjunction with Cosmic Explorer will be able to identify and characterize most binary coalescence events, subtract them from the data, and potentially measure the underlying primordial background (although the accumulation of the errors in the subtraction of resolved sources will also produce an important foreground [642, 643, 2453], see also section 10.5.3).

JCAP03(2026)081

Several mechanisms that generate stochastic GW background produce a spectrum that extends over many decades in frequency. The use of observatories operating in very different frequency bands is then crucial for characterizing them (as well as for increasing the confidence in a detection). Working with PTAs, the 10-year long GAIA database, LISA, as well as with Deci-Hz detectors, ET could help understand stochastic backgrounds over six orders of magnitude in frequency range from nanohertz to kilohertz. In this section, we explore the synergies between ET and LISA (section 6.7.1), and ET and PTA (section 6.7.2) towards the aim of a joint detection of the cosmological SGWB.

6.7.1 Synergies between ET and LISA

Although ET and LISA operate across different frequency ranges, both are expected to have comparable integrated sensitivities to the amplitude of a SGWB. In this subsection we explore the potential synergies between these two observatories for analyzing GW sources from the early Universe that generate a SGWB with a high amplitude and a broad frequency spectrum. In combining the results of LISA and ET, we are able to cover a much larger range of frequencies, of order

$$\mathcal{O}(10^{-5})\,\mathrm{Hz} \leq f \leq \mathcal{O}(10^{3})\,\mathrm{Hz}\,. \tag{6.1}$$

As discussed in section 3.2, SGWB sources that could produce an observable stochastic GW signal in this range include first order phase transitions, cosmic strings, and inflation (beyond single-field slow roll). For such broad signals, combining data from both LISA and ET offers a clearer signal characterisation and more precise extraction of physical properties than using either instrument alone, since we can study the signal across the full frequency band in eq. (6.1).

We analyse this possibility using Fisher forecasts to assess the detectability of the SGWB shape in synergy among the two instruments. We consider a Gaussian likelihood on the GW energy density $\Omega_{\rm GW}$ with a covariance matrix given by a combination of the nominal sensitivity curves for LISA [647] and ET in its triangle configuration. The Fisher plots are produced using the `GetDist` package [2580]. For the theoretical SGWB frequency profile, a useful SGWB template is the broken power law (BPL) function. This model provides a good first approximation for GW spectra generated by various early Universe phenomena [2581]. We follow ref. [702] for the form of the BPL function

$$\Omega^{\rm th}_{\rm GW}(f) = \Omega_\star \left(\frac{f}{f_\star}\right)^{n_1} \left[\frac{1}{2} + \frac{1}{2}\left(\frac{f}{f_\star}\right)^{\sigma}\right]^{\frac{n_2-n_1}{\sigma}}\,, \tag{6.2}$$

where $f_\star$ determines the break position, and $\Omega_\star$ is the amplitude of the spectrum at the break. The parameters n_1 and n_2 correspond to the spectral indices before and after the break, while σ controls the break's smoothness. We use the BBN bound $\Omega_{\rm GW} \leq 1.7 \times 10^{-6}$ [691] as the reference for the SGWB's maximal amplitude, even when considering post-BBN sources. The previous profile will be applied to investigate GW from phase transitions and cosmic strings; a different, log-normal Ansatz will be considered for the case of inflation. We show in figure 117 the benchmark scenarios for the examples we are going to discuss next, together with the nominal and power law sensitivity curves for LISA, and for ET in the triangle

JCAP03(2026)081

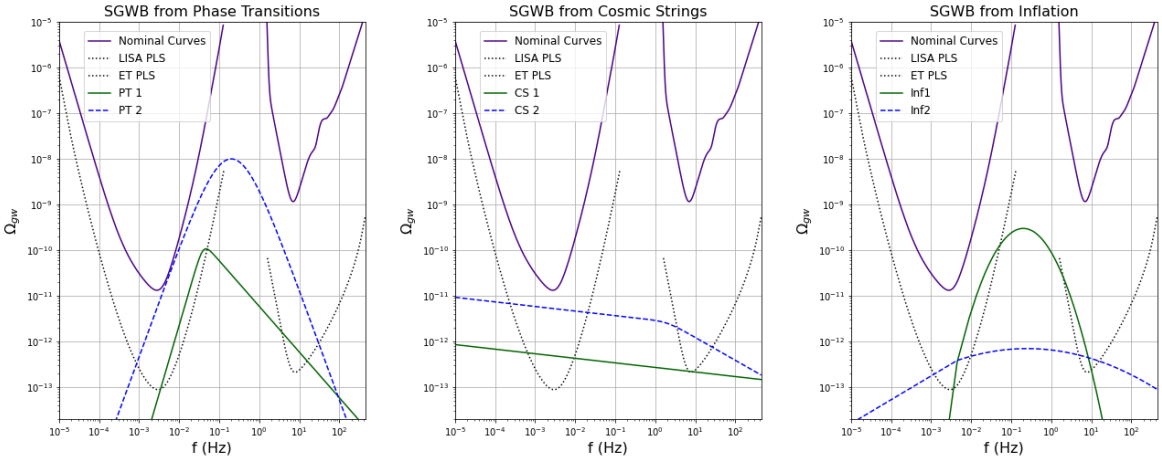

Figure 117. *Left panel:* examples of SGWB from phase transitions (PT). *Middle panel:* examplexs of SGWB from cosmic strings (CS). *Right panel:* examples of SGWB from cosmic inflation. Besides LISA and ET sensitivity curves (PSD) and the corresponding PLS (see eq. (3.21) and section 10.5.2 for definitions), in blue and green lines are represented the benchmark scenarios discussed in each of the aforementioned sections. See ref. [2605]. Reprinted figure with permission from [2605], Copyright (2025) by the American Physical Society.

	$\Omega_\star$	n_1	n_2	σ	$f_\star$
PT1	1×10^{-10}	3	-1	7.2	0.04
PT2	1×10^{-8}	2.4	-2.4	1.2	0.2
CS1	4×10^{-13}	-0.1	-0.1	–	0.02
CS2	2.5×10^{-12}	-0.1	$-\frac{1}{2}$	3	2

	$\Omega_\star$	$f_\star$	ρ
Inf1	3×10^{-10}	0.2	0.45
Inf2	7×10^{-13}	0.25	1.6

Table 11. *Left:* benchmark values associated with Ansatz (6.2) for the scenarios corresponding to cosmological phase transitions and cosmic string models. *Right:* benchmark values for cosmological inflation scenarios described by Ansatz (6.3). See ref. [2605]. Reprinted figure with permission from [2605], Copyright (2025) by the American Physical Society.

configuration (using the ET-D sensitivity curve).[59] For more details about our scenarios and our methods of analysis, see ref. [2582].

Phase transitions. The production of stochastic GW background from phase transitions has been discussed in section 3.2.2. In particular, in the GWs produced by bubble collisions, the SGWB follows the BPL profile [702], as in eq. (6.2) or similar parametrizations such as eq. (3.46). Other mechanisms that produce GWs from PTs, such as sound waves in primordial plasma [2583, 2584] and turbulent motion [2585–2587], rather follow a double broken power-law profile, see [702]. However, the focus here is on the overall structure across the broad frequency band in eq. (6.1), and so we use the BPL template eq. (6.2) as a reasonable approximation.

[59] See figure 195 for the ET PLS with the updated sensitivity curve used in [16] as well as for the PLS of the 2L configurations, with different relative angles and arm lengths.

JCAP03(2026)081

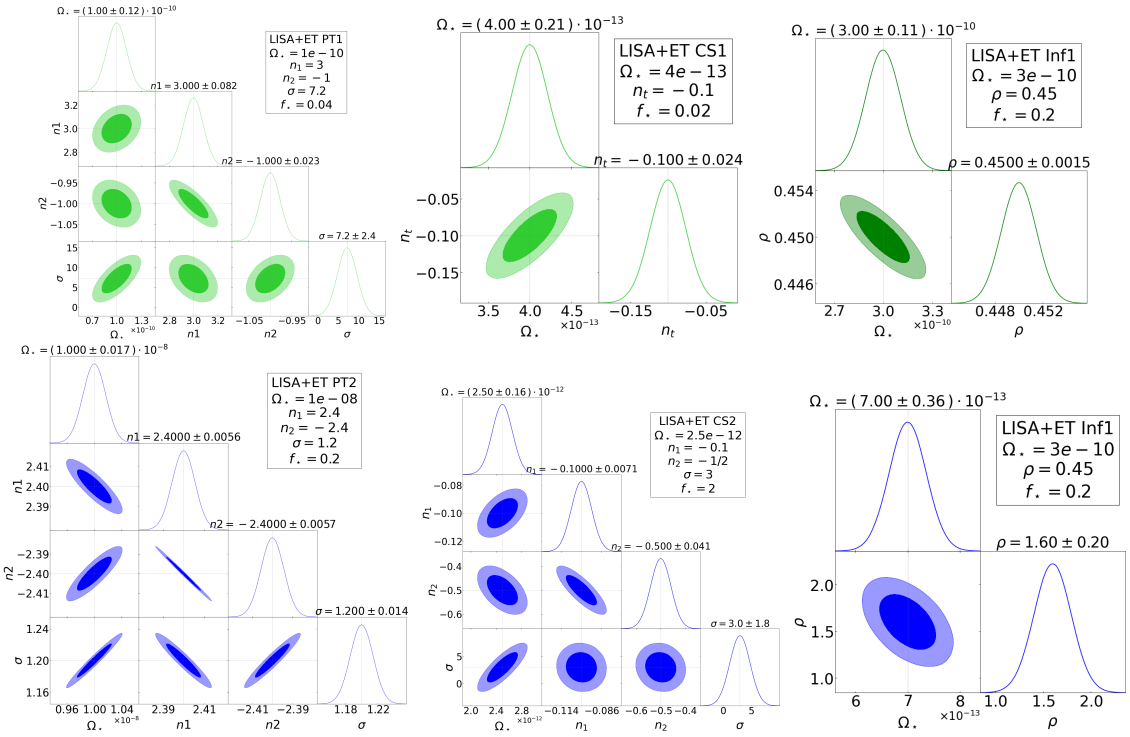

Figure 118. First and second column: Fisher forecasts for the phase transition and cosmic string scenarios. Third column: Fisher forecasts for the inflation benchmark scenarios. See table 11. See ref. [2605]. Reprinted figure with permission from [2605], Copyright (2025) by the American Physical Society.

We consider the scenarios in table 11: scenario PT1 has spectral index $n_1 = 3$ in the infrared [1019] and $n_2 = -1$ in the UV. This scenario matches cases where GWs are produced by sound waves of the bubble surrounding plasma, or by effects of turbulent behavior in the fluid. For the second benchmark scenario, PT2, we consider the model of ref. [757] in the context of highly relativistic fluid shell dynamics, which finds $n_1 = -n_2 \simeq 2.4$ and $\sigma \simeq 1.2$. These scenarios are shown in the left panel of figure 117. Notice that the SGWB amplitude is well below the nominal sensitivity curves (i.e. the Power Spectral Density, PSD): nevertheless, the SGWB can be detected with a sufficient signal-to-noise ratio by integrating over frequencies. In fact, in all panels of figure 117, besides the PSD, we also include the power-law integrated sensitivity curves (PLS) introduced in ref. [564] (see also section 10.5.2), which exploit the aforementioned integration over frequencies. In plotting the curves, we assume three years of observation, and we take a threshold of detection corresponding to SNR= 5.

For both scenarios PT1 and PT2 in figure 118, LISA and ET individually can accurately measure only one of the spectral indices n_1 or n_2 (for more details and additional Fisher plots comparing different cases, see ref. [2582]). However, the two experiments together can measure both quantities with at least 10% accuracy. The parameter σ, which controls the smoothness of the transition, can also be measured more precisely with combined data. This highlights that using LISA and ET together provides richer insights into high-temperature PT physics, also reducing parameter degeneracies.

JCAP03(2026)081

Cosmic strings. As discussed in section 3.2.3, cosmic strings form networks where interactions create loops of varying sizes, which decay and generate a SGWB spanning a broad frequency range. Determining the spectral tilts n_1, n_2 and the break position will provide insights into both the cosmic string properties and the Universe's evolution before BBN. In fact, by analysing the spectrum's frequency profile, we can also be able to constrain non-standard pre-BBN cosmic epochs. For normal cosmological expansions, we expect the SGWB from cosmic strings to approximately follow a power law profile in the band of eq. (6.1): this corresponds to our benchmark scenario CS1 of table 11 (see e.g. ref. [2581]). We obtain the values for the benchmark scenario CS2 from [2588], corresponding to a spectral tilt being dependent on the equation of state w in a non-standard cosmological expansion, where $n_2 = -2(3w-1)/(3w+1)$ for values where $w \geq 1/4$. The middle panel of figure 117 illustrates the benchmark values used in our CS cases. Only with both instruments together can the full set of parameters be measured within 10% accuracy. See figure 118, middle column, and ref. [2582] for more details.

Cosmic inflation. As discussed in section 3.2.1, see in particular figure 26 while the most minimal inflation models based on single-field slow-roll predict a SGWB amplitude too small for both ET and LISA to detect, several well-motivated scenarios can boost the amplitude to observable levels within the frequency band given by eq. (6.1). These scenarios include dynamics of vector and axion fields [601, 603]; spontaneous space-time symmetry breaking [2589–2591]; and effects associated with the production of primordial black holes [1013, 1014]. Generally, a SGWB from inflation exhibits a more complex frequency profile than those from other sources, potentially featuring log-normal shapes, multiple peaks, or oscillatory patterns (see ref. [648] for a discussion of various inflation templates.). We consider the so-called log-normal peak Ansatz:

$$\Omega_{\rm GW} = \Omega_\star \exp\left\{\left[-\frac{\ln^2\left(f/f_\star\right)}{2\rho^2}\right]\right\}, \tag{6.3}$$

where $\Omega_\star$, $f_\star$, and ρ control the amplitude, position, and smoothness of the peak. This scenario can be the result of axion or axion spectator inflation models [608, 611, 688]. Table 11 gives the values used in our benchmark scenarios, which are also shown in the right panel of figure 117. The corresponding Fisher forecasts are presented in figure 118, third column. Particularly for scenario Inf2 we learn there are significant benefits from the combining the results of the two instruments for reducing the errors in the measurements (again see ref. [2582] for a more detailed analysis).

6.7.2 Synergies between ET and PTAs

A primordial SGWB can span a large range of frequencies, from Cosmic Microwave Background frequencies of 10^{-17} Hz, Pulsar Timing Array (PTA) frequencies of around 10^{-9} Hz, LISA frequencies in the milli-Hertz range as well as ground-based observatories above a few Hz and up to a few kHz. ET observations can thus be studied in synergy with CMB, PTA and LISA observations. Specific scenarios are however different for each type of cosmological background, e.g. inflation, first-order phase transitions, cosmic strings, domain walls or second-order scalar perturbations associated with primordial black holes: see for example figure 17 of [2592].

JCAP03(2026)081

Single field slow-roll inflation is detectable by CMB instruments such as Planck at the lowest frequencies, but its red tilt implies that it cannot be detected by either PTAs, LISA or ET, see figure 26. However, as we discussed in section 3.2.1 other, more complex inflationary scenarios can produce a GW spectrum with a positive spectral index n_t (blue tilt), making them potentially detectable by PTAs, LISA and ET. Ref. [2593] used actual CMB, PTA and LIGO measurements to place constraints on a SGWB of inflationary origin, in particular on n_t and the tensor-to-scalar ratio r (characterizing the amplitude of a primordial GW signal as compared to the amplitude of scalar perturbations as detected in the CMB). This is an example of how different instruments across the GW spectrum can be used to place constraints on a SGWB.

More recently, in 2023, PTA results across the globe have shown evidence for a SGWB [2594–2598]. Work is in progress to confirm these results with a 5σ significance. If confirmed as a true SGWB, the most likely source is a background of supermassive black holes. In this case, because of the completely different masses, there would be little synergy between PTAs and ET (but there would be synergy between PTAs and LISA in the sense that PTA sources can inform expected LISA findings on massive black hole binaries). However, another possible source is a cosmological background. In refs. [421, 809], the observed signal was interpreted as a cosmological background and the spectral index n_t and tensor-to-scalar ratio r were estimated. While, in principle, these estimates could be used to search for this same background in the ET data, the observed spectral index in PTA data is quite high and not compatible with the high frequencies of ET if the spectral index is assumed to be fixed; however, in the case of a running index across GW frequencies, a PTA background could be compatible with a background in ET. Another possibility is a non-conventional cosmological history with a period characterised by a stiff equation of state [1074]. Additionally, a CMB detection of a GW background would be groundbreaking; a combined detection of a primordial SGWB in both the CMB and PTA data could make it easier to find the same signal in ET. However, it is much more likely that in PTA data, the cosmological background is present as a secondary background with a foreground of supermassive black hole binaries. Work is ongoing to model a search for both backgrounds. Cosmic strings, domain walls, first-order phase transitions and second-order perturbations or Primordial black holes (PBH) could also be detected by PTAs, LISA and ET. The recent PTA results [421, 809] are not compatible with a cosmic string signal, but are potentially compatible with a first-order phase transition or PHBs. Ref. [2599] looked at the combined NANOGrav and EPTA results and their possible interpretation as a cosmological background. Many papers on the interpretation of PTA results as a cosmological background have in fact been published after the June 2023 release of results by the main PTA collaborations, and trying to summarize them all is a research avenue in and of itself.

In conclusion, PTA data can help inform an ET search for a cosmological background. On the one hand, PTA data can help constrain a SGWB in the nanohertz GW frequency range, as the sensitivity of PTAs improves, in particular in light of the upcoming Square Kilometre Array. Recent results (from 2023) provide evidence for a correlated common red noise that could be a SGWB that is compatible with a background generated in exotic inflationary scenarios, first-order phase transitions or second-order scalar perturbations, but

JCAP03(2026)081

requires in each case a surprisingly large effect. More probably, the cosmological background is only secondary to a foreground of supermassive black holes, in which the spectral index of the cosmological background would be lower and thus more compatible with a similar index at high ET frequencies. Studying scenarios of running spectral indices across the GW frequency range as well as differing equations of state are good avenues for linking the PTA frequencies with the ET frequencies and thus finding synergies.

Take home message

- Possible early Universe GW sources can provide a SGWB profile spanning many decades in frequency: cosmic phase transitions, cosmic strings, and cosmic inflation.
- SGWB from primordial sources have a rich frequency dependence, whose characterization improves up to a 10% accuracy by means of a multiband detection by ET and by other GW detectors.
- Synergies between ET and other GW instruments thus provide invaluable information on primordial sources of the SGWB, and on the early history of our Universe expansion.

6.8 Executive summary

In this section we have explored how the science case of ET is enhanced by exploiting synergies with other GW observatories, operating either in a similar frequency band, as Cosmic Explorer, or in completely different bands, as LISA, deciHz detectors such as LGWA, or PTA.

Joint observations of ET with Cosmic Explorer will consolidate the science of this emerging and transformative field. The synergy with lower-frequency GW observatories, such as PTA at nHz, LISA in the mHz bandwidth, and design concepts like LGWA in the deciHz interval, will broaden the scientific case for ET. These synergies allows for connections to be made with other GW sources also in different astrophysical environments, enabling the investigation of some of the most compelling questions in astrophysics, physics and cosmology. In particular:

Synergies of ET with other GW observatories:

- Synergies between CE and ET enable a more comprehensive exploration of the Universe by extending further the cosmic horizon (see figure 105), enlarging the search for intermediate-mass black holes — an entirely uncharted territory — and enhancing the accuracy of measurements of the source's physical parameters, resolving degeneracies and obtaining a comprehensive and robust understanding of the nature of neutron stars and black holes.
- Joint observations of ET with CE offer a unique opportunity to measure the GW polarization modes and constrain alternative gravity theories. The dipolar radiation test is significantly enhanced by combining ET with milli-Hertz and Deci-hertz gravitational wave detectors.

JCAP03(2026)081

- 3rd-generation observatories like ET and CE will be the only observatories capable of discovering the relics of the first massive stars expected to form during cosmic dawn. These observatories will provide better measurements of the masses and redshifts of these black holes, shedding light on the formation of pristine stars in binaries. Some of these black holes could serve as "light" seeds for the growth of massive black holes.
- The collaboration between ET and CE represents a transformative advancement for late-time cosmology with resolved sources, due to the improved localization capabilities that are critical for both bright and dark siren cosmology. Furthermore, the synergy with other gravitational wave observatories, such as LISA, will expand the range of GW sources available.
- Multi-wavelength observations of merging black holes, captured by LISA in their early inspiral phase and by ET at the point of merger, are crucial for understanding the formation pathways of stellar-mass and intermediate-mass binary black holes. The combined observations of these systems by ET and LISA can further constrain General Relativity (GR) with an order of magnitude better precision than either observatory could achieve alone.
- BBHs originating from massive stars with masses in the range $120M_\odot - 300M_\odot$, are prime candidates for GW observations across multiple frequency bands. The prolonged inspiral signals emitted by these systems can be observed by LISA and by Deci-Hz detectors, while the later stages of inspiral and merger will be detected by ET. The combination of the observations from LISA or from Deci-Hz detectors such as LGWA, with the ET observations will dramatically improve the sky localization of these sources, making them effective dark sirens for the determination of cosmological parameters.
- By comparing merger events detected by ET and LISA, which are sensitive to different mass ranges (around $100\,M_\odot$ for ET and $10^5\,M_\odot$ for LISA), we can gain statistical insight into the mechanisms behind black hole seeding and growth.
- Intermediate mass ratio inspiral, where a stellar mass BHs merges with an intermediate mass black hole (IMBH), are exquisite probes of the physics of formation of IMBH in dense environments. Combining observations from ET, LGWA and LISA makes it possible to cover the IMBH mass range fully and to place stringent constraints on the IMBH mass distribution, shedding light on their origin, see figure 116.
- GW sources from the early Universe, such as cosmic phase transitions, cosmic strings, and cosmic inflation, may provide a stochastic gravitational wave background (SGWB) profile across multiple frequency bands. The SGWB from primordial sources has a rich frequency dependence, which can be characterized with up to 10% accuracy through multi-band detection by ET and other GW

JCAP03(2026)081

detectors such as LISA, detectors operating in the deciHz such as LGWA, and PTA. Consequently, synergies between ET and other instruments offer invaluable information about primordial sources of the SGWB and the early history of the Universe's expansion.

- A confident detection of a stochastic GW background requires control of correlated noise among the detectors involved in the correlation (the two distant detectors in the ET-2L configuration, the three colocated detectors in the ET-triangle configuration, and the three independent channels of LISA). Bringing in fully independent observatories, such as CE on the ground, or TianQin and Taiji in space, provides more robust detection prospects. Cross-correlating data from distant sites eliminates (or, on ground, further reduces) the possibility of correlated environmental or instrumental disturbances (see sections 3.1.5, 3.1.6 and 11.6.2 for discussions), yielding a far more robust claim of correlated signal, rather than just an excess of correlated broadband noise. At the same time, each new baseline adds signal-to-noise, improving overall sensitivity.

7 Subatomic Physics with ET

The first detection of GWs from a merging neutron star binary system and the accompanying observations of electromagnetic counterparts in 2017 demonstrated the enormous potential of multi-messenger astronomy for nuclear physics. Neutron stars comprise the highest densities of matter that can stably exist in the Universe. The gravitational-wave signals emitted from events involving neutron stars encode detailed and clean information on the dense matter in their interiors and, for a subset of binary neutron star mergers, on the subatomic microphysics in regimes of yet higher density and temperature. Such invaluable insights into states of subatomic matter under extreme conditions are inaccessible to any other probes and, in conjunction with electromagnetic counterparts, enable a multitude of additional opportunities, such as understanding the nucleosynthesis of very heavy elements. This section emphasizes the advances in nuclear and neutron star physics poised to open up with future gravitational-wave detections by ET, which are synergistic yet go beyond what can be accomplished with other astrophysical and terrestrial experiments. We also advocate progress in microscopic nuclear and hadron theory to fully exploit ET and test gravity in the regime of largest achievable densities and pressures, that of neutron stars.

7.1 Introduction

Astrophysical environments involving neutron stars (NSs) — objects where gravity compresses matter to several times the normal nuclear density — are unique testbeds for a rich variety of subatomic physics. A NS encompasses different phases of matter over a large range in density: from neutron-rich nuclei and free electrons in the outer parts to a uniform liquid of primarily neutrons, until the densities become so high in the very cores that other particles may be populated such as hyperons or mesons, which could also form condensates, and/or a transition to degenerate quark matter. This is illustrated in figure 119 and makes NSs

JCAP03(2026)081